ÉCOLE POLYTECHNIQUE FÉDÉRALE DE LAUSANNE

MATHICSE

Mathematics Institute of Computational Science and Engineering

School of Basic Sciences - Section of Mathematics

MATHICSE Technical Report

Nr. 32.2012

August 2012

Analysis and computation of the elastic wave equation with random coefficients

M. Motamed, F. Nobile, R. Tempone

http://mathicse.epfl.ch

Phone: +41 21 69 37648

Address:
EPFL - SB - MATHICSE (Bâtiment MA)
Station 8 - CH-1015 - Lausanne - Switzerland

Fax: +41 21 69 32545

Analysis and computation of the elastic wave equation with random coefficients

Mohammad Motamed[♯⋆] Fabio Nobile[†‡] Raúl Tempone[♯]

August 23, 2012

[♯] King Abdullah University of Science and Technology, 4700 KAUST, Jeddah, Saudi Arabia
mohammad.motamed@kaust.edu.sa raul.tempone@kaust.edu.sa

[⋆] Institute for Computational Engineering and Sciences, University of Texas Austin, TX 78712, USA

[†] MATHICSE-CSQI, École Polytechnique Fédérale de Lausanne Station 8, CH-1015 Lausanne, Switzerland
fabio.nobile@epfl.ch

[‡] MOX, Dipartimento di Matematica "F. Brioschi", Politecnico di Milano via Bonardi 9, 20133 Milano, Italy

Keywords: uncertainty quantification; stochastic partial differential equations; elastic wave equation; regularity; collocation method; error analysis.

AMS Subject Classification: 65C20 65M70 65M60 65M06 65M15 65Z05

Abstract

We analyze the stochastic initial-boundary value problem for the elastic wave equation with random coefficients and deterministic data. We propose a stochastic collocation method for computing statistical moments of the solution or statistics of some given quantities of interest. We study the convergence rate of the error in the stochastic collocation method. In particular, we show that, the rate of convergence depends on the regularity of the solution or the quantity of interest in the stochastic space, which is in turn related to the regularity of the deterministic data in the physical space and the type of the quantity of interest. We demonstrate that a fast rate of convergence is possible in two cases: for the elastic wave solutions with high regular data; and for some high regular quantities of interest even in the presence of low regular data. We perform numerical examples, including a simplified earthquake, which confirm the analysis and show that the collocation method is a valid alternative to the more traditional Monte Carlo sampling method for problems with high stochastic regularity.

1 Introduction

The elastic wave equation describes phenomena such as seismic waves in the earth and ultrasound waves in elastic materials. It is a system of linear second order hyperbolic partial differential equations (PDEs) in a two or three dimensional physical space and has a more complex form than the standard acoustic wave equation, as it accounts for both longitudinal and transverse motions. There can also be surface waves traveling along a free surface, as well as waves that travel along internal material discontinuities.

It is often desirable to include uncertainty in the PDE models and quantify its effects on the predicted solution or other quantities of physical interest. The uncertainty may be either due to the lack of knowledge (systematic uncertainty), or due to inherent variations of the physical system (statistical uncertainty). In earthquake modeling, for instance, seismic waves propagate in a geological region where, due to soil spatial variability and the uncertainty of measured soil parameters, both kinds of uncertainties are present.

Probability theory provides an effective tool to describe and propagate uncertainty. It parametrizes the uncertain input data either in terms of a finite number of random variables or more generally by random fields. Several techniques are available for solving PDEs in probabilistic setting. The most frequently used technique is the Monte Carlo sampling [9] which features a very slow convergence rate. Other recent approaches, which in certain situations feature a much faster convergence rate, include Stochastic Galerkin [11, 25, 45, 1, 37] and Stochastic Collocation [2, 29, 30, 44]. Such methods are based on global polynomials and exploit the possible regularity that the solution might have with respect to the input parameters to yield a very fast convergence.

For stochastic elliptic and parabolic problems, under particular assumptions, the solution is analytic with respect to the input random parameters [2, 28, 6]. Consequently, Stochastic Galerkin and Stochastic Collocation methods can be successfully applied to such problems due to the fast decay of the error as a result of the high stochastic regularity. For stochastic hyperbolic problems, the regularity analysis is more involved. For the one-dimensional scalar advection equation with a time- and space-independent random wave speed, it is shown that the solution possess high regularity provided the data live in suitable spaces [43, 12, 36]. The main difficulty, however, arises when the coefficients vary in space or time. Recently, in [26], we have studied the second order acoustic wave equation with discontinuous random wave speeds. We have shown that unlike in elliptic and parabolic problems, the solution to hyperbolic problems is not in general analytic with respect to the random variables. Therefore, the rate of convergence may only be algebraic. However, a fast rate of convergence is still possible for some quantities of interest and for the wave solution with particular types of data. For the more difficult case of stochastic nonlinear conservation laws, where the corresponding regularity theory is lacking, we refer to the computational studies in [21, 22, 33, 40, 41].

In this work, we consider the elastic wave equation in a random heterogeneous medium with time-independent and smooth material properties, augmented with de-

terministic initial data and source terms and subject to different types of boundary conditions. In particular, we are interested in low-to-moderate frequency seismic waves propagating in slowly varying underlying media. We therefore assume that the wave length is not very small compared to the overall size of the domain and is comparable to the scale of the variations in the medium. We study the well-posedness and stochastic regularity of the problem by employing the energy method, which is based on the weak formulation of the problem and integration by parts. The main result of this paper, presented in Theorems 4.2, 4.3, 4.4, 4.5, is that the regularity of the solution or the quantity of interest in the stochastic space is closely related to the regularity of the deterministic data in the physical space and the type of the quantity of interest. We demonstrate that high stochastic regularity is possible in two cases: for the elastic wave solutions with high regular data; and for some high regular physical quantities of interest even in the presence of low regular data. For such problems, a fast spectral convergence is therefore possible when a stochastic collocation method is employed.

The outline of the paper is as follows: in Section 2 we formulate the mathematical problem and establish the main assumptions. The well-posedness of the problem is studied in Section 3. In Section 4, we provide regularity results on the solution and some physical quantities of interest. The collocation method for solving the underlying stochastic PDE and the related error convergence results are addressed in Section 5. In Section 6 we perform some numerical examples. Finally, we present our conclusions in Section 7.

2 Problem statement

Let D be an open bounded subset of $\mathbb{R}^d$, $d = 2, 3$, with a smooth boundary ∂D, and $(\Omega, \mathcal{F}, P)$ be a complete probability space. Here, Ω is the set of outcomes, $\mathcal{F} \subset 2^\Omega$ is the σ-algebra of events and $P : \mathcal{F} \to [0, 1]$ is a probability measure. Consider the stochastic initial boundary value problem (IBVP): find a random vector-valued function $\mathbf{u} : [0, T] \times \bar{D} \times \Omega \to \mathbb{R}^d$, such that P-almost everywhere in Ω, i.e. almost surely (a.s), the following holds:

$$\nu(\mathbf{x}, \omega)\, \mathbf{u}_{tt}(t, \mathbf{x}, \omega) - \nabla \cdot \boldsymbol{\sigma}(\mathbf{u}(t, \mathbf{x}, \omega)) = \mathbf{f}(t, \mathbf{x}) \quad \text{in } [0, T] \times D \times \Omega, \tag{1a}$$

$$\mathbf{u}(0, \mathbf{x}, \omega) = \mathbf{g}_1(\mathbf{x}), \qquad \mathbf{u}_t(0, \mathbf{x}, \omega) = \mathbf{g}_2(\mathbf{x}) \qquad \text{on } \{t = 0\} \times D \times \Omega, \tag{1b}$$

$$\boldsymbol{\sigma}(\mathbf{u}(t, \mathbf{x}, \omega)) \cdot \hat{\mathbf{n}} = \mathbf{h}(t, \mathbf{x}) \qquad \text{on } [0, T] \times \partial D \times \Omega. \tag{1c}$$

Here, the stress tensor is

$$\boldsymbol{\sigma}(\mathbf{u}) = \lambda(\mathbf{x}, \omega)\, \nabla \cdot \mathbf{u}\, I + \mu(\mathbf{x}, \omega)\, (\nabla \mathbf{u} + (\nabla \mathbf{u})^\top), \tag{2}$$

with $\mathbf{u} = (u_1, \ldots, u_d)^\top$ being the displacement vector, t and $\mathbf{x} = (x_1, \ldots, x_d)^\top$ are the time and location, respectively, and I is the identity matrix. A non-homogeneous Neumann (or normal stress or traction) boundary condition (1c) is imposed on the boundary ∂D, where $\hat{\mathbf{n}}$ is the outward unit normal to the boundary. When $\mathbf{h} = 0$, it is called a stress-free boundary condition. We will also address other types of boundary

conditions including non-homogeneous Dirichlet and absorbing boundary conditions (see Section 3.3).

We take the external forcing, initial data, and boundary force term as

$$\begin{aligned} &\mathbf{f} \in \mathbf{L}^2((0,T);\mathbf{L}^2(D)), && \mathbf{h} \in \mathbf{L}^2((0,T);\mathbf{H}^{1/2}(\partial D)), \\ &\mathbf{g}_1 \in \mathbf{H}^1(D), && \mathbf{g}_2 \in \mathbf{L}^2(D), \end{aligned} \tag{3}$$

The precise definition of these real vector-valued function spaces will be given in Section 3.

The material properties are characterized by the density ν and the Lamé parameters λ and μ that define the stress tensor (2). We consider a heterogeneous medium and assume that these parameters are random and $\mathbf{x}$-smooth, i.e.,

$$\nu(.,\omega),\ \lambda(.,\omega),\ \mu(.,\omega) \in C^\infty(D), \quad \text{a.s.} \tag{4}$$

This regularity may be relaxed, see for instance Remark 4.1. We also assume that the parameters are uniformly bounded and coercive, and therefore the following inequalities hold:

$$0 < \nu_{min} \leq \nu(\mathbf{x},\omega) \leq \nu_{max} < \infty, \quad \forall\, \mathbf{x} \in D, \quad \text{a.s,} \tag{5a}$$
$$0 < \lambda_{min} \leq \lambda(\mathbf{x},\omega) \leq \lambda_{max} < \infty, \quad \forall\, \mathbf{x} \in D, \quad \text{a.s,} \tag{5b}$$
$$0 < \mu_{min} \leq \mu(\mathbf{x},\omega) \leq \mu_{max} < \infty, \quad \forall\, \mathbf{x} \in D, \quad \text{a.s.} \tag{5c}$$

The system (1) admits longitudinal (P or pressure) and transverse (S or shear) waves which, in the case of constant density, propagate at phase velocities $c_p = \sqrt{(2\,\mu + \lambda)/\nu}$, and $c_s = \sqrt{\mu/\nu}$, respectively. There can also be surface waves traveling along a free surface, as well as waves that travel along internal material discontinuities.

We further make the following *finite dimensional noise* assumption on the form of the coefficients,

$$\nu(\mathbf{x},\omega) = \nu(\mathbf{x}, Y_1(\omega), \ldots, Y_N(\omega)), \quad \forall\, \mathbf{x} \in D, \quad \text{a.s,} \tag{6a}$$
$$\lambda(\mathbf{x},\omega) = \lambda(\mathbf{x}, Y_1(\omega), \ldots, Y_N(\omega)), \quad \forall\, \mathbf{x} \in D, \quad \text{a.s,} \tag{6b}$$
$$\mu(\mathbf{x},\omega) = \mu(\mathbf{x}, Y_1(\omega), \ldots, Y_N(\omega)), \quad \forall\, \mathbf{x} \in D, \quad \text{a.s,} \tag{6c}$$

where $N \in \mathbb{N}_+$ and $Y = [Y_1, \ldots, Y_N] \in \mathbb{R}^N$ is a random vector. We denote by $\Gamma_n \equiv Y_n(\Omega)$ the image of each component Y_n and assume that Y_n is bounded for $n = 1, \ldots, N$. We let $\Gamma = \prod_{n=1}^N \Gamma_n$ and assume further that the random vector Y has a bounded joint probability density function $\rho : \Gamma \to \mathbb{R}_+$ with $\rho \in L^\infty(\Gamma)$.

The finite dimensional noise assumption implies that the solution of the stochastic IBVP (1) can be described by only N random variables,

$$\mathbf{u}(t,\mathbf{x},\omega) = \mathbf{u}(t,\mathbf{x}, Y_1(\omega), \ldots, Y_N(\omega)).$$

This turns the original stochastic problem into a deterministic IBVP for the elastic wave equation with an N-dimensional parameter, which allows the use of standard

finite difference and finite element methods to approximate the solution of the resulting deterministic problem $\mathbf{u} = \mathbf{u}(t, \mathbf{x}, Y)$, where $t \in [0, T]$, $\mathbf{x} \in D$, and $Y \in \Gamma$. Note that the knowledge of $\mathbf{u} = \mathbf{u}(t, \mathbf{x}, Y)$ fully determines the law of the random field $\mathbf{u} = \mathbf{u}(t, \mathbf{x}, \omega)$. The ultimate goal is then the prediction of statistical moments of the solution or statistics of some given quantities of physical interest.

In this work, we consider $\mathbf{x}$-smooth random parameters (4) with bounded mixed Y-derivatives of any order. Therefore, for a multi-index $\mathbf{k} \in \mathbb{N}^N$ with $|\mathbf{k}| \geq 0$, we assume

$$\|\partial_Y^{\mathbf{k}} \nu\|_{L^\infty(D)},\ \|\partial_Y^{\mathbf{k}} \lambda\|_{L^\infty(D)},\ \|\partial_Y^{\mathbf{k}} \mu\|_{L^\infty(D)} < \infty, \quad \forall\, Y \in \Gamma. \tag{7}$$

For instance, the random coefficients may be given linearly in Y by

$$\nu(\mathbf{x}, \omega) = \hat{\nu}_0(\mathbf{x}) + \sum_{n=1}^{N} \hat{\nu}_n(\mathbf{x})\, Y_n(\omega), \tag{8a}$$

$$\lambda(\mathbf{x}, \omega) = \hat{\lambda}_0(\mathbf{x}) + \sum_{n=1}^{N} \hat{\lambda}_n(\mathbf{x})\, Y_n(\omega), \tag{8b}$$

$$\mu(\mathbf{x}, \omega) = \hat{\mu}_0(\mathbf{x}) + \sum_{n=1}^{N} \hat{\mu}_n(\mathbf{x})\, Y_n(\omega), \tag{8c}$$

where $\hat{\nu}_i$, $\hat{\lambda}_i$ and $\hat{\mu}_i$, with $i = 0, 1, \ldots, N$, are smooth functions defined everywhere in D, and Y_n are independent and identically distributed random variables. A typical example is when the random field $\nu(\mathbf{x}, \omega)$ is approximated by a truncated Karhunen-Loéve expansion with N terms. We note that, in this case, the covariance function should be such that the corresponding eigenfunctions are smooth. For simplicity, and without loss of generality, the proof of regularity results in the stochastic space are given for linear coefficients (8). The regularity results hold true for general coefficients satisfying (4)-(7). We will address the cases of discontinuous and piecewise $\mathbf{x}$-smooth random parameters elsewhere. See also our work in [26] on the acoustic wave equation with discontinuous random coefficients.

3 Well-posedness

The well-posedness theory of linear hyperbolic IBVPs is well developed for many classes of first and second order systems with different types of non-homogeneous boundary conditions, including Dirichlet, Neumann, Robin, and absorbing-type boundary conditions involving time derivatives. This general theory is based on a variety of mathematical techniques, such as the energy integral method, Laplace-Fourier transform, the construction of symmetrizers, and the theory of pseudo-differential operators [15, 17, 23, 24, 14, 20].

In this section, we will address the well-posedness of the stochastic IBVP (1) with the data satisfying (3) and the coefficients satisfying (4)-(6).

3.1 Function spaces

We first define function spaces that we need in this work. For a real vector-valued function $\mathbf{v}(Y) = (v_1(Y), \ldots, v_d(Y))^\top \in \mathbb{R}^d$ of the random vector $Y \in \Gamma$, we define the space of square integrable functions:

$$\mathbf{L}^2_\rho(\Gamma) = \{\mathbf{v} : \Gamma \to \mathbb{R}^d, \int_\Gamma \sum_{i=1}^d |v_i(Y)|^2 \, \rho(Y) \, dY < \infty\},$$

endowed with the inner product

$$(\mathbf{v}, \mathbf{u})_{L^2_\rho(\Gamma)} = \sum_{i=1}^d \mathbb{E}\left[v_i \, u_i\right] = \int_\Gamma \sum_{i=1}^d v_i \, u_i \, \rho(Y) \, dY.$$

For a real vector-valued function $\mathbf{v}(\mathbf{x}) \in \mathbb{R}^d$ of $\mathbf{x} \in D$, we define the Sobolev space $\mathbf{H}^k(D)$ for integer order $k \geq 0$:

$$\mathbf{H}^k(D) = \{\mathbf{v} : D \to \mathbb{R}^d, \int_D \sum_{i=1}^d |\partial^\alpha_{\mathbf{x}} v_i(\mathbf{x})|^2 \, d\mathbf{x} < \infty, \, \forall \alpha, \, |\alpha| \leq k\},$$

where $\alpha = (\alpha_1, \ldots, \alpha_d) \in \mathbb{Z}^d_+$ is a multi-index with $|\alpha| = \alpha_1 + \ldots + \alpha_d$, and $\partial^\alpha_{\mathbf{x}} := \frac{\partial^{|\alpha|}}{\partial^{\alpha_1}_{x_1} \ldots \partial^{\alpha_d}_{x_d}}$. Naturally, $\mathbf{H}^k(D)$ is a Hilbert space with the inner product

$$(\mathbf{v}, \mathbf{u})_{\mathbf{H}^k(D)} = \int_D \sum_{|\alpha| \leq k} \sum_{i=1}^d \partial^\alpha_{\mathbf{x}} v_i(\mathbf{x}) \, \partial^\alpha_{\mathbf{x}} u_i(\mathbf{x}) \, d\mathbf{x}.$$

For the particular case of $k = 0$, we obtain the space of square integrable vector-valued functions $\mathbf{L}^2(D) = \mathbf{H}^0(D)$. The space $\mathbf{H}^{-k}(D)$ is the dual of $\mathbf{H}^k(D)$. We also define the space $\mathbf{H}^k_0(D)$ as the closure of the space of smooth functions with compact support $\mathbf{C}^\infty_0(D)$ in $\mathbf{H}^k(D)$.

Now let $\mathbf{H}^k(D) \otimes \mathbf{L}^2_\rho(\Gamma)$ be a tensor space with tensor inner product

$$(\mathbf{v}, \mathbf{u})_{\mathbf{H}^k(D) \otimes \mathbf{L}^2_\rho(\Gamma)} = \int_\Gamma \int_D \sum_{|\alpha| \leq k} \sum_{i=1}^d \partial^\alpha_{\mathbf{x}} v_i(\mathbf{x}) \, \partial^\alpha_{\mathbf{x}} u_i(\mathbf{x}) \, d\mathbf{x} \, \rho(Y) \, dY.$$

Thus, if $\mathbf{v} \in \mathbf{H}^k(D) \otimes \mathbf{L}^2_\rho(\Gamma)$, then $\mathbf{v}(\mathbf{x}, .) \in \mathbf{L}^2_\rho(\Gamma)$ a.e. on D and $\mathbf{v}(., Y) \in \mathbf{H}^k(D)$ a.e. on Γ. We then introduce the mapping $\mathbf{u} : [0, T] \to \mathbf{H}^k(D) \otimes \mathbf{L}^2_\rho(\Gamma)$, defined by

$$[\mathbf{u}(t)](\mathbf{x}, Y) := \mathbf{u}(t, \mathbf{x}, Y), \quad \forall \, t \in [0, T], \, \mathbf{x} \in D, \, Y \in \Gamma.$$

In other words, we view the function $\mathbf{u}(t, \mathbf{x}, Y)$ as a function of t with values $\mathbf{u}(t)$ in the Hilbert space $\mathbf{H}^k(D) \otimes \mathbf{L}^2_\rho(\Gamma)$. Similarly, we introduce the function $\mathbf{f} : [0, T] \to \mathbf{H}^k(D)$, defined by

$$[\mathbf{f}(t)](\mathbf{x}) := \mathbf{f}(t, \mathbf{x}), \quad \forall \, t \in [0, T], \, \mathbf{x} \in D.$$

Finally, for a real Hilbert space $\mathbf{H}^k(D)$ equipped with the norm $\|\mathbf{v}\|_{\mathbf{H}^k(D)} = (\mathbf{v},\mathbf{v})^{1/2}_{\mathbf{H}^k(D)}$, we introduce the time-involving space $\mathbf{L}^2((0,T);\mathbf{H}^k(D)\otimes\mathbf{L}^2_\rho(\Gamma))$, consisting of all measurable vector-valued functions $\mathbf{v}$ with

$$\int_{[0,T]\times\Gamma} \|\mathbf{v}\|^2_{\mathbf{H}^k(D)}\,\rho(Y)\,dY\,dt < \infty.$$

Similarly, for the Hilbert space $\mathbf{V} = \mathbf{H}^k(D)\otimes\mathbf{L}^2_\rho(\Gamma)$, we denote by $\mathbf{C}^m([0,T];\mathbf{V})$, with $m = 0, 1, \ldots$, the space of all m times continuously differentiable functions defined on $[0,T]$ with values in $\mathbf{V}$.

3.2 Weak formulation

Because of the assumptions on the data (3), we need to interpret (1) in the distributional sense and consider a weak formulation of the problem. We therefore consider

$$\int_{[0,T]\times D\times\Gamma} \big(\nu\,\mathbf{u}'' - \nabla\cdot\boldsymbol{\sigma}(\mathbf{u})\big)\cdot\mathbf{v}\,\rho\,dY\,d\mathbf{x}\,dt = \int_{[0,T]\times D\times\Gamma} \mathbf{f}\cdot\mathbf{v}\,\rho\,dY\,d\mathbf{x}\,dt,$$

for all test functions $\mathbf{v} \in \mathbf{C}^\infty_0([0,T];\mathbf{H}^1(D)\otimes\mathbf{L}^2_\rho(\Gamma))$. Integration by parts in space gives us

$$\int_{[0,T]\times D\times\Gamma} \big(\nu\,\mathbf{u}''\cdot\mathbf{v} + \nabla\mathbf{v} : \boldsymbol{\sigma}(\mathbf{u})\big)\,\rho\,dY\,d\mathbf{x}\,dt = \int_{[0,T]\times\partial D\times\Gamma} \mathbf{v}\cdot\boldsymbol{\sigma}(\mathbf{u})\cdot\hat{\mathbf{n}}\,\rho\,dY\,d\mathbf{x}\,dt + \int_{[0,T]\times D\times\Gamma} \mathbf{f}\cdot\mathbf{v}\,\rho\,dY\,d\mathbf{x}\,dt, \quad (9)$$

where the tensor contraction on tensors A and B is defined by $A : B = \sum_{i,j} A_{ij}\,B_{ij}$. We first notice that $\boldsymbol{\sigma}(\mathbf{u})\cdot\hat{\mathbf{n}}$ is well-defined on the boundary ∂D, see Appendix B.2 of [14] and [35]. For instance, in $\mathbb{R}^2$, the domain D may locally be considered as the half-plane $\mathbb{R}^2_0 = \{\mathbf{x} = (x_1,x_2)^\top : x_2 \geq 0, -\infty < x_1 < \infty\}$ with the boundary $\partial D = \{x_2 = 0\}$, for which $\hat{\mathbf{n}} = [0,-1]^\top$. Then, one can show that $\boldsymbol{\sigma}(\mathbf{u})\cdot\hat{\mathbf{n}}$ is a continuous function of x_2 with values in $\mathbf{H}^{-1}((0,T)\times\mathbb{R})\otimes\mathbf{L}^2_\rho(\Gamma)$, and therefore, the restriction to $\{x_2 = 0\}$ is a well defined distribution. We also note that for the normal stress boundary condition (1c), we have $\boldsymbol{\sigma}(\mathbf{u})\cdot\hat{\mathbf{n}} = \mathbf{h}$ on the boundary. We then define the notion of weak solutions to the stochastic IBVP (1).

Definition 3.1 *For the stochastic IBVP* (1) *with the data satisfying* (3) *and coefficients satisfying* (4)-(6)*, the function* $\mathbf{u} \in \mathbf{L}^2((0,T);\mathbf{H}^1(D)\otimes\mathbf{L}^2_\rho(\Gamma))$ *with* $\mathbf{u}' \in \mathbf{L}^2((0,T);\mathbf{L}^2(D)\otimes\mathbf{L}^2_\rho(\Gamma))$ *and* $\mathbf{u}'' \in \mathbf{L}^2((0,T);\mathbf{H}^{-1}(D)\otimes\mathbf{L}^2_\rho(\Gamma))$ *is a weak solution provided the following hold:*

(i) $\mathbf{u}(0) = \mathbf{g}_1$ *and* $\mathbf{u}'(0) = \mathbf{g}_2$,

(ii) for all test functions $\mathbf{v} \in \mathbf{C}_0^\infty([0,T];\mathbf{H}^1(D)\otimes\mathbf{L}^2_\rho(\Gamma))$*:*

$$\int_{[0,T]\times D\times\Gamma} \left(\nu\,\mathbf{u}''\cdot\mathbf{v} + \nabla\mathbf{v} : \boldsymbol{\sigma}(\mathbf{u})\right)\,\rho\,dY\,d\mathbf{x}\,dt = \int_{[0,T]\times\partial D\times\Gamma} \mathbf{v}\cdot\mathbf{h}\,\rho\,dY\,d\mathbf{x}\,dt + \int_{[0,T]\times D\times\Gamma} \mathbf{f}\cdot\mathbf{v}\,\rho\,dY\,d\mathbf{x}\,dt. \quad (10)$$

Note that since $\mathbf{u}'' \in \mathbf{L}^2((0,T);\mathbf{H}^{-1}(D)\otimes\mathbf{L}^2_\rho(\Gamma))$, then $\mathbf{u}' \in \mathbf{H}^1((0,T);\mathbf{H}^{-1}(D)\otimes\mathbf{L}^2_\rho(\Gamma))$ and therefore $\mathbf{u}' \in \mathbf{C}^0([0,T];\mathbf{H}^{-1}(D)\otimes\mathbf{L}^2_\rho(\Gamma))$, see Theorem 5 in Section 5.9.2 in [8]. Similarly, we have $\mathbf{u} \in \mathbf{C}^0([0,T];\mathbf{L}^2(D)\otimes\mathbf{L}^2_\rho(\Gamma))$. Therefore, $\mathbf{u}(0)$ and $\mathbf{u}'(0)$ in (i) are well-defined. We note that, due to (2), we have $\nabla\mathbf{v} : \boldsymbol{\sigma}(\mathbf{u}) = \lambda\,(\nabla\cdot\mathbf{v})\,(\nabla\cdot\mathbf{u}) + \mu\,\nabla\mathbf{v} : (\nabla\mathbf{u} + (\nabla\mathbf{u})^\top)$.

We have the following result on the existence and uniqueness of the weak solution.

Theorem 3.1 *Consider the Stochastic IBVP* (1) *with data satisfying* (3) *and random parameters satisfying* (4), (5), *and* (6). *There exists a unique weak solution* $\mathbf{u} \in \mathbf{C}^0([0,T];\mathbf{H}^1(D)\otimes\mathbf{L}^2_\rho(\Gamma)) \cap \mathbf{C}^1([0,T];\mathbf{L}^2(D)\otimes\mathbf{L}^2_\rho(\Gamma)) \cap \mathbf{H}^2((0,T);\mathbf{H}^{-1}(D)\otimes\mathbf{L}^2_\rho(\Gamma))$ *to the problem which depends continuously on the data.*

Proof. The proof is an easy extension of the proof for deterministic problems [23]. □

Remark 3.1 *We note that the assumption on the regularity of the boundary term* $\mathbf{h}$ *in* (3) *is not sharp. We can obtain the same regularity of the weak solution by imposing weaker assumptions. The result of Theorem 3.1 remains true if we assume* $\mathbf{h} \in \mathbf{L}^2((0,T);\mathbf{H}^{2/5+\epsilon}(\partial D))$, $\forall\epsilon > 0$ *[19]. For the purposes of this work however assumption* (3) *suffices.*

Remark 3.2 *A similar result as in Theorem 3.1 can be obtained pointwise in* $Y \in \Gamma$. *In this case we interpret the solution* $\mathbf{u}(t,\mathbf{x},Y)$ *as a Hilbert-valued function on* Γ,

$$\mathbf{u} = \mathbf{u}(Y) : \Gamma \to \mathbf{C}^0([0,T];\mathbf{H}^1(D)) \cap \mathbf{C}^1([0,T];\mathbf{L}^2(D)) \cap \mathbf{H}^2((0,T);\mathbf{H}^{-1}(D)).$$

Such function is uniformly bounded on Γ *thanks to assumptions* (5).

3.3 Boundary conditions

So far, we have studied the non-homogeneous Neumann boundary condition (1c). In this section, we address two other types of boundary conditions: non-homogeneous Dirichlet and absorbing boundary conditions.

3.3.1 Non-homogneous Dirichlet boundary conditions

Consider the stochastic IBVP (1) with the boundary condition (1c) replaced by

$$\mathbf{u}(t,\mathbf{x},\omega) = \mathbf{h}^D(t,\mathbf{x}) \qquad \text{on } [0,T]\times\partial D\times\Omega, \quad (11)$$

with $\mathbf{h}^D \in \mathbf{L}^2((0,T);\mathbf{H}^1(\partial D))$. By an easy extension of the proof of Theorem 24.1.1 in [14] we can show that Theorem 3.1 also holds for the stochastic problem (1a)-(1b) with the boundary condition (11).

3.3.2 Absorbing boundary conditions

We now consider a boundary condition of the form

$$\mathbf{u}_t = M\,\boldsymbol{\sigma}(\mathbf{u})\cdot\hat{\mathbf{n}}, \tag{12}$$

where M is a given matrix in $\mathbb{R}^{d\times d}$ independent of $\mathbf{u}$. We assume that enough regularity is present so that the terms $\mathbf{u}_t$ and $\boldsymbol{\sigma}(\mathbf{u})\cdot\hat{\mathbf{n}}$ are well-defined on the boundary. It is easy to observe that the time variation of the energy

$$E(t) = \frac{1}{2}\int_{D\times\Gamma}\left(\nu\,|\mathbf{u}'|^2 + \lambda\,|\nabla\cdot\mathbf{u}|^2 + 2\,\mu\,\left|\frac{\nabla\mathbf{u}+(\nabla\mathbf{u})^\top}{2}\right|^2\right)\rho\,dY\,d\mathbf{x},$$

is given by

$$\frac{d}{dt}E(t) = \int_{\partial D\times\Gamma}\mathbf{u}'\cdot\boldsymbol{\sigma}(\mathbf{u})\cdot\hat{\mathbf{n}}\;\rho\,dY\,d\mathbf{x} + \int_{D\times\Gamma}\mathbf{f}\cdot\mathbf{u}'\,\rho\,dY\,d\mathbf{x}. \tag{13}$$

In particular, when $\mathbf{f}=\mathbf{0}$, for the boundary condition of type (12), we obtain from (13)

$$\frac{d}{dt}E(t) = \int_{\partial D\times\Gamma} M^{-1}\;\mathbf{u}'\cdot\mathbf{u}'\;\rho\,dY\,d\mathbf{x}. \tag{14}$$

Therefore, any boundary condition (12) with a negative definite matrix M results in a non-increasing energy and hence a well-posed problem. Such types of boundary conditions are called energy absorbing conditions. They are dissipative as they make the right hand side of (14) negative. In a two-dimensional physical space, for instance, for a boundary given by $x_1 = 0$, a class of Clayton-Engquist boundary conditions [5, 31] is obtained by setting

$$M = -\begin{bmatrix} \frac{1}{\sqrt{\nu\,(2\,\mu+\lambda)}} & 0 \\ 0 & \frac{1}{\sqrt{\nu\,\mu}} \end{bmatrix}. \tag{15}$$

Such absorbing boundary conditions (12) with (15) are very important in wave propagation problems, as they reduce the non-physical reflections of outgoing waves from artificial boundaries used to truncate the computational domain.

4 Stochastic regularity

In this section we study the regularity of the solution and some quantities of interest with respect to the random input variable Y. As it will be shown, the Y-regularity is closely related to the regularity of data in time and space. The ultimate use of Y-regularity in obtaining convergence rate of the error for the stochastic collocation method will be discussed in the next section.

4.1 Stochastic regularity of the solution

Let the data in (1) satisfy

$$\begin{aligned} &\mathbf{f} \in \mathbf{L}^2((0,T);\mathbf{H}^s(D)), && \mathbf{h} \in \mathbf{L}^2((0,T);\mathbf{H}^{s+1/2}(\partial D)),\\ &\mathbf{g}_1 \in \mathbf{H}^{s+1}(D), && \mathbf{g}_2 \in \mathbf{H}^s(D), \end{aligned} \tag{16}$$

where s is an integer with $s \geq -1$. When $s \geq 1$, we further assume the following *compatibility conditions*,

$$\boldsymbol{\sigma}(\mathbf{g}_1(\mathbf{x})) \cdot \hat{\mathbf{n}} = \mathbf{h}(0,\mathbf{x}), \qquad \boldsymbol{\sigma}(\mathbf{g}_2(\mathbf{x})) \cdot \hat{\mathbf{n}} = \partial_t \mathbf{h}(0,\mathbf{x}), \qquad \mathbf{x} \in \partial D. \tag{17}$$

We notice that for the low regular cases when $s = -1, 0$, the compatibility conditions are not required to achieve the optimal regularity in the solution [23, 24, 19, 20].

We first state the main result on the time and space regularity of the solution:

Theorem 4.1 *Consider the stochastic IBVP* (1) *with data given by* (16)-(17) *and with random coefficients satisfying* (4)-(7)*. Then there is a unique weak solution*

$$\mathbf{u}(.,Y) \in \mathbf{C}^0([0,T];\mathbf{H}^{s+1}(D)) \cap \mathbf{C}^1([0,T];\mathbf{H}^s(D)) \cap \mathbf{H}^2((0,T);\mathbf{H}^{s-1}(D)), \quad \forall\, Y \in \Gamma, \tag{18}$$

which is uniformly bounded in Γ *and depends continuously on the data.*

Proof. The proof is an easy extension of the proofs in [23, 24, 19]. □

In other words, in the interior, the solution $\mathbf{u}$ gains *half a derivative* in space over the Neumann boundary force term $\mathbf{h}$ and *one derivative* in space over the force term $\mathbf{f}$. We note that in [19] sharper estimates are obtained improving the "$\frac{1}{2}$ gain" regularity to "$\frac{3}{5} - \epsilon$ gain" regularity with $\epsilon > 0$.

To study the Y-regularity of the solution, we k-times differentiate (1), with $k \geq 1$, with respect to Y_n and obtain

$$\nu\, \partial^k_{Y_n} \mathbf{u}_{tt} - \nabla \cdot \boldsymbol{\sigma}(\partial^k_{Y_n} \mathbf{u}) = k\, \nabla \cdot \tilde{\boldsymbol{\sigma}}(\partial^{k-1}_{Y_n} \mathbf{u}) - k\, \partial_{Y_n} \nu\, \partial^{k-1}_{Y_n} \mathbf{u}_{tt} =: \mathbf{f}^{(k)}, \tag{19a}$$

$$\mathbf{u}(0,\mathbf{x},Y) = \mathbf{0}, \qquad \mathbf{u}_t(0,\mathbf{x},Y) = \mathbf{0}, \tag{19b}$$

$$\boldsymbol{\sigma}(\partial^k_{Y_n} \mathbf{u}) \cdot \hat{\mathbf{n}} = -k\, \tilde{\boldsymbol{\sigma}}(\partial^{k-1}_{Y_n} \mathbf{u}) \cdot \hat{\mathbf{n}} =: \mathbf{h}^{(k)}, \tag{19c}$$

where

$$\tilde{\boldsymbol{\sigma}}(\mathbf{v}) := (\partial_{Y_n} \lambda)\ \nabla \cdot \mathbf{v}\, I + (\partial_{Y_n} \mu)\ (\nabla \mathbf{v} + (\nabla \mathbf{v})^\top). \tag{20}$$

We note that since the coefficients are linear in Y, as in (8), their second and higher Y-derivatives are zero. This however imposes no restriction. In fact, for nonlinear coefficients in Y, the right hand side of (19a) may have additional terms containing Y-derivatives of $\mathbf{u}$ of order less than $k-1$. We also note that the following divergence formula for integration by parts holds,

$$\begin{aligned} \int_D \mathbf{v} \cdot \nabla \cdot \boldsymbol{\sigma}(\mathbf{u})\, d\mathbf{x} &= -\int_D \nabla \mathbf{v} : \boldsymbol{\sigma}(\mathbf{u})\, d\mathbf{x} + \int_{\partial D} \mathbf{v} \cdot \boldsymbol{\sigma}(\mathbf{u}) \cdot \hat{\mathbf{n}}\, d\mathbf{x} = \\ &= \int_D \mathbf{u} \cdot \nabla \cdot \boldsymbol{\sigma}(\mathbf{v})\, d\mathbf{x} - \int_{\partial D} \mathbf{u} \cdot \boldsymbol{\sigma}(\mathbf{v}) \cdot \hat{\mathbf{n}}\, d\mathbf{x} + \int_{\partial D} \mathbf{v} \cdot \boldsymbol{\sigma}(\mathbf{u}) \cdot \hat{\mathbf{n}}\, d\mathbf{x}. \end{aligned} \tag{21}$$

We now prove the following result on the Y-regularity of the solution.

Theorem 4.2 *For the solution of the stochastic IBVP* (1) *with data given by* (16)-(17) *and with random coefficients satisfying* (4)-(7)*, we have for* $0 \le k \le s+1$*,*

$$\partial_{Y_n}^k \mathbf{u}(.,Y) \in \mathbf{C}^0([0,T];\mathbf{H}^{s+1-k}(D)), \qquad \forall\, Y \in \Gamma, \tag{22}$$

and uniformly bounded in Γ*.*

Proof. The case $k=0$ corresponds to Theorem 4.1. Now let $k \ge 1$. We use induction on $1 \le k \le s+1$.

Case $k=1$**.** In this case $s \ge 0$. First let $s=0$. Due to low regularity of the data, we consider (19) in the weak form. From (19a), with $k=1$, and the divergence formula (21), we obtain $\forall\, Y \in \Gamma$,

$$\int_{[0,T]\times D} \nu\, \partial_{Y_n}\mathbf{u}'' \cdot \mathbf{v}\, d\mathbf{x}\, dt + \int_{[0,T]\times D} \nabla\mathbf{v} : \boldsymbol{\sigma}(\partial_{Y_n}\mathbf{u})\, d\mathbf{x}\, dt - \int_{[0,T]\times \partial D} \mathbf{v}\cdot\boldsymbol{\sigma}(\partial_{Y_n}\mathbf{u})\cdot\hat{\mathbf{n}}\, d\mathbf{x}\, dt =$$
$$- \int_{[0,T]\times D} \nabla\mathbf{v} : \tilde{\boldsymbol{\sigma}}(\mathbf{u})\, d\mathbf{x}\, dt + \int_{[0,T]\times \partial D} \mathbf{v}\cdot\tilde{\boldsymbol{\sigma}}(\mathbf{u})\cdot\hat{\mathbf{n}}\, d\mathbf{x}\, dt - \int_{[0,T]\times D} \partial_{Y_n}\nu\, \mathbf{u}''\cdot\mathbf{v}\, d\mathbf{x}\, dt,$$

$\forall\, \mathbf{v} \in \mathbf{L}^2((0,T);\mathbf{H}^1(D))$. Using the boundary condition (19c), we arrive at

$$\int_{[0,T]\times D} \nu\, \partial_{Y_n}\mathbf{u}'' \cdot \mathbf{v}\, d\mathbf{x}\, dt + \int_{[0,T]\times D} \nabla\mathbf{v} : \boldsymbol{\sigma}(\partial_{Y_n}\mathbf{u})\, d\mathbf{x}\, dt =$$
$$- \int_{[0,T]\times D} \nabla\mathbf{v} : \tilde{\boldsymbol{\sigma}}(\mathbf{u})\, d\mathbf{x}\, dt - \int_{[0,T]\times D} \partial_{Y_n}\nu\, \mathbf{u}''\cdot\mathbf{v}\, d\mathbf{x}\, dt. \tag{23}$$

The right hand side of (23) is a linear functional of $\mathbf{v}$,

$$\mathbf{f}^*(\mathbf{v}) := - \int_{[0,T]\times D} \nabla\mathbf{v} : \tilde{\boldsymbol{\sigma}}(\mathbf{u})\, d\mathbf{x}\, dt - \int_{[0,T]\times D} \partial_{Y_n}\nu\, \mathbf{u}''\cdot\mathbf{v}\, d\mathbf{x}\, dt,$$

with bounded $\mathbf{L}^2((0,T);\mathbf{H}^{-1}(D))$ norm:

$$\sup_{\mathbf{v}\in\mathbf{L}^2((0,T);\mathbf{H}^1(D))} \frac{|\mathbf{f}^*(\mathbf{v})|}{||\mathbf{v}||_{\mathbf{L}^2((0,T);\mathbf{H}^1(D))}} < \infty,$$

due to (7) and (18) for $s=0$ and noticing that $\tilde{\boldsymbol{\sigma}}(\mathbf{u})$, given by (20), is linear with respect to $\nabla\mathbf{u}$. Therefore, comparing (23) with (10), we can consider $\partial_{Y_n}\mathbf{u}$ as the weak solution of a problem of type (1) with a force term in $\mathbf{L}^2((0,T);\mathbf{H}^{-1}(D))$ and homogeneous initial and boundary data. Employing Theorem 4.1, we obtain (22) for $k=1$ and $s=0$ uniformly in Γ. In other words, $\partial_{Y_n}\mathbf{u}$ gains one derivative over the force term and lies in the space $\mathbf{L}^2((0,T);\mathbf{L}^2(D))$.

Now let $s \ge 1$. By (18) and noticing that $\tilde{\boldsymbol{\sigma}}(\mathbf{u})$ is linear with respect to $\nabla\mathbf{u}$ and employing the trace theorem, we have

$$\mathbf{f}^{(1)} \in \mathbf{L}^2((0,T);\mathbf{H}^{s-1}(D)), \qquad \mathbf{h}^{(1)} \in \mathbf{L}^2((0,T);\mathbf{H}^{s-1/2}(\partial D)).$$

Therefore, by Theorem 4.1 we get (22) with k=1.

General case. We now assume that (22) holds for $1 \le k = k_0 \le s$. We want to show that it also holds for $2 \le k = k_0+1 \le s+1$, that is,

$$\partial_{Y_n}^{k_0+1} \mathbf{u}(.,Y) \in \mathbf{C}^0([0,T];\mathbf{H}^{s-k_0}(D)), \qquad \forall\, Y \in \Gamma. \tag{24}$$

For this, we need first to show that

$$\mathbf{f}^{(k_0+1)} \in \mathbf{L}^2((0,T);\mathbf{H}^{s-k_0-1}(D)), \qquad \mathbf{h}^{(k_0+1)} \in \mathbf{L}^2((0,T);\mathbf{H}^{s-k_0-1/2}(\partial D)), \tag{25}$$

and then employ Theorem 4.1 to arrive at (24). But (25) follows by the induction hypothesis and using the same approach as in the case when $k = 1$, by considering two cases: when $s - k_0 = 0$, and when $s - k_0 \geq 1$. This completes the proof. □

We now consider the mixed Y-derivatives of the solution and state the following result.

Theorem 4.3 *For the solution of the stochastic IBVP* (1) *with data given by* (16)-(17) *and with random coefficients satisfying* (4)-(7)*, we have for a multi-index* $\mathbf{k} \in \mathbb{N}^N$ *with* $0 \leq |\mathbf{k}| \leq s+1$,

$$\partial_Y^{\mathbf{k}}\mathbf{u}(.,Y) := \frac{\partial^{|\mathbf{k}|}}{\partial_{Y_1}^{k_1}\dots\partial_{Y_N}^{k_N}}\mathbf{u}(.,Y) \in \mathbf{C}^0([0,T];\mathbf{H}^{s+1-|\mathbf{k}|}(D)), \qquad \forall\, Y \in \Gamma, \tag{26}$$

and uniformly bounded in Γ.

Proof. The proof is an easy modification of the proof of Theorem 6 in [26]. □

Remark 4.1 *The smoothness assumption in* (4) *may be relaxed to a weaker assumption. In fact, we can obtain the same regularity results stated in Theorems 4.1, 4.2 and 4.3 with the coefficients* ν, λ *and* μ *belonging to* $C^s(D)$ *almost surely.*

4.2 Stochastic regularity of quantities of interest

4.2.1 Mollified solutions

Consider the quantity of interest

$$\mathcal{Q}(Y) = \int_0^T \int_D \mathbf{u}(t,\mathbf{x},Y)\cdot\boldsymbol{\phi}(\mathbf{x})\,d\mathbf{x}\,dt, \tag{27}$$

where $\mathbf{u}$ solves (1) and $\boldsymbol{\phi} \in \mathbf{H}^k(D)$ is a vector-valued mollifier with $k \in \mathbb{N}$ being a non-negative integer. Moreover, we let the data in (1) satisfy (16)-(17) with $s \in \mathbb{N}$. We want to investigate the Y-regularity of (27).

We first introduce the *influence function* (or dual solution) $\boldsymbol{\varphi}$ associated to the quantity of interest, $\mathcal{Q}$, as the solution of the dual problem

$$\nu(\mathbf{x},Y)\,\boldsymbol{\varphi}_{tt}(t,\mathbf{x},Y) - \nabla\cdot\boldsymbol{\sigma}(\boldsymbol{\varphi}(t,\mathbf{x},Y)) = \boldsymbol{\phi}(\mathbf{x}) \quad \text{in } [0,T]\times D\times\Gamma \tag{28a}$$

$$\boldsymbol{\varphi}(T,\mathbf{x},Y) = \mathbf{0}, \qquad \boldsymbol{\varphi}_t(T,\mathbf{x},Y) = \mathbf{0} \qquad \text{on } \{t=T\}\times D\times\Gamma \tag{28b}$$

$$\boldsymbol{\sigma}(\boldsymbol{\varphi}(t,\mathbf{x},Y))\cdot\hat{\mathbf{n}} = \mathbf{0} \qquad \text{on } [0,T]\times\partial D\times\Gamma \tag{28c}$$

We note that this is a well-posed backward elastic equation with zero data at the final time T and a time-independent force term. By Theorem 4.1 and Theorem 4.2, the dual solution $\boldsymbol{\varphi}$ satisfies

$$\boldsymbol{\varphi}(.,Y) \in \mathbf{C}^0([0,T];\mathbf{H}^{k+1}(D)), \qquad \partial_{Y_n}^{k+1}\boldsymbol{\varphi}(.,Y) \in \mathbf{C}^0([0,T];\mathbf{L}^2(D)), \qquad \forall\, Y\in\Gamma,$$

with uniform norms in Γ. We further note that, since the coefficients and data in (28) are time-independent, the above regularity results hold also for all time derivatives of $\boldsymbol{\varphi}$.

We now s-times differentiate (1a) with respect to Y_n and obtain, thanks to (8),

$$\nu\, \partial_{Y_n}^s \mathbf{u}_{tt} - \nabla \cdot \boldsymbol{\sigma}(\partial_{Y_n}^s \mathbf{u}) = s\, \nabla \cdot \tilde{\boldsymbol{\sigma}}(\partial_{Y_n}^{s-1} \mathbf{u}) - s\, \partial_{Y_n} \nu\, \partial_{Y_n}^{s-1} \mathbf{u}_{tt}, \tag{29}$$

where $\tilde{\boldsymbol{\sigma}}$ is given by (20). We are now ready to prove the following result.

Theorem 4.4 *Let $k, s \in \mathbb{N}$ be two non-negative integers. Moreover, assume that $\boldsymbol{\phi} \in \mathbf{H}^k(D)$. Then, under the assumptions* (16)-(17) *and for linear coefficients of type* (8) *satisfying* (4)-(7)*, the Y-derivatives of the quantity of interest* (27) *are given by*

$$\begin{aligned} d_{Y_n}^{s+k+1} \mathcal{Q}(Y) = {} & C_{s,k} \int_0^T \int_D \nabla \partial_{Y_n}^k \boldsymbol{\varphi} : \tilde{\boldsymbol{\sigma}}(\partial_{Y_n}^s \mathbf{u})\, d\mathbf{x}\, dt \\ & + C_{s,k} \int_0^T \int_D \partial_{Y_n} \nu\, \partial_{Y_n}^k \boldsymbol{\varphi}_{tt} \cdot \partial_{Y_n}^s \mathbf{u}\, d\mathbf{x}\, dt \\ & + C_{s,k} \int_D \partial_{Y_n} \nu \left[\partial_{Y_n}^k \boldsymbol{\varphi}(0, \mathbf{x}, Y) \cdot \partial_{Y_n}^s \mathbf{g}_2(\mathbf{x}) - \partial_{Y_n}^k \boldsymbol{\varphi}_t(0, \mathbf{x}, Y) \cdot \partial_{Y_n}^s \mathbf{g}_1(\mathbf{x}) \right] d\mathbf{x}, \end{aligned} \tag{30}$$

where $C_{s,k} = \frac{-1}{k!} \prod_{\ell=1}^{k+1} (s + \ell)$.

Proof. We prove (30) by induction on $k \geq 0$.
Case $k = 0$. In this case, we $s + 1$ times differentiate (27) with respect to Y_n and use (28a). We have for every $s \geq 0$,

$$\begin{aligned} d_{Y_n}^{s+1} \mathcal{Q}(Y) &= \int_0^T \int_D \partial_{Y_n}^{s+1} \mathbf{u} \cdot \boldsymbol{\phi}\, d\mathbf{x}\, dt = \\ &= \int_0^T \int_D \partial_{Y_n}^{s+1} \mathbf{u} \cdot \left(\nu\, \boldsymbol{\varphi}_{tt} - \nabla \cdot \boldsymbol{\sigma}(\boldsymbol{\varphi}) \right) d\mathbf{x}\, dt = \\ &= \int_0^T \int_D \nu\, \partial_{Y_n}^{s+1} \mathbf{u} \cdot \boldsymbol{\varphi}_{tt}\, d\mathbf{x}\, dt - \int_0^T \int_D \boldsymbol{\varphi} \cdot \nabla \cdot \boldsymbol{\sigma}(\partial_{Y_n}^{s+1} \mathbf{u})\, d\mathbf{x}\, dt \\ &\quad + \int_0^T \int_{\partial D} \boldsymbol{\varphi} \cdot \boldsymbol{\sigma}(\partial_{Y_n}^{s+1} \mathbf{u}) \cdot \hat{\mathbf{n}}\, d\mathbf{x} - \int_0^T \int_{\partial D} \partial_{Y_n}^{s+1} \mathbf{u} \cdot \boldsymbol{\sigma}(\boldsymbol{\varphi}) \cdot \hat{\mathbf{n}}\, d\mathbf{x}, \end{aligned} \tag{31}$$

where the last equality follows by the second equality in (21). We now use (29) and note that by (28c), the last term in (31) is zero. Moreover, by (1c), we have $\boldsymbol{\sigma}(\partial_{Y_n}^{s+1} \mathbf{u}) \cdot \hat{\mathbf{n}} + (s+1)\, \tilde{\boldsymbol{\sigma}}(\partial_{Y_n}^s \mathbf{u}) \cdot \hat{\mathbf{n}} =$

0 on the boundary. Then

$$
\begin{aligned}
d_{Y_n}^{s+1}\mathcal{Q}(Y) &= \int_0^T \int_D \nu\, \partial_{Y_n}^{s+1}\mathbf{u}\cdot\boldsymbol{\varphi}_{tt}\, d\mathbf{x}\, dt \\
&\quad - \int_0^T \int_D \boldsymbol{\varphi}\cdot\Big(\nu\, \partial_{Y_n}^{s+1}\mathbf{u}_{tt} - (s+1)\,\nabla\cdot\tilde{\boldsymbol{\sigma}}(\partial_{Y_n}^{s}\mathbf{u}) + (s+1)\,\partial_{Y_n}\nu\, \partial_{Y_n}^{s}\mathbf{u}_{tt}\Big)\, d\mathbf{x}\, dt \\
&\quad - (s+1)\int_0^T \int_{\partial D} \boldsymbol{\varphi}\cdot\tilde{\boldsymbol{\sigma}}(\partial_{Y_n}^{s}\mathbf{u})\cdot\hat{\mathbf{n}}\, d\mathbf{x}, \\
&= \int_0^T \int_D \nu\left(\partial_{Y_n}^{s+1}\mathbf{u}\cdot\boldsymbol{\varphi}_{tt} - \boldsymbol{\varphi}\cdot\partial_{Y_n}^{s+1}\mathbf{u}_{tt}\right) d\mathbf{x}\, dt \\
&\quad - (s+1)\int_0^T \int_D \nabla\boldsymbol{\varphi} : \tilde{\boldsymbol{\sigma}}(\partial_{Y_n}^{s}\mathbf{u})\, d\mathbf{x}\, dt - (s+1)\int_0^T \int_D \partial_{Y_n}\nu\, \boldsymbol{\varphi}\cdot\partial_{Y_n}^{s}\mathbf{u}_{tt}\, d\mathbf{x}\, dt,
\end{aligned}
$$

where the last equality follows by the first equality in (21) with $\boldsymbol{\sigma}$ replaced by $\tilde{\boldsymbol{\sigma}}$. By integration by parts in t, we therefore obtain

$$
\begin{aligned}
d_{Y_n}^{s+1}\mathcal{Q}(Y) &= -(s+1)\int_0^T \int_D \nabla\boldsymbol{\varphi} : \tilde{\boldsymbol{\sigma}}(\partial_{Y_n}^{s}\mathbf{u})\, d\mathbf{x}\, dt - (s+1)\int_0^T \int_D \partial_{Y_n}\nu\, \boldsymbol{\varphi}_{tt}\cdot\partial_{Y_n}^{s}\mathbf{u}\, d\mathbf{x}\, dt \\
&\quad - (s+1)\int_D \partial_{Y_n}\nu\left[\boldsymbol{\varphi}\cdot\partial_{Y_n}^{s}\mathbf{u}_t - \boldsymbol{\varphi}_t\cdot\partial_{Y_n}^{s}\mathbf{u}\right]_0^T d\mathbf{x} = \\
&= -(s+1)\int_0^T \int_D \nabla\boldsymbol{\varphi} : \tilde{\boldsymbol{\sigma}}(\partial_{Y_n}^{s}\mathbf{u})\, d\mathbf{x}\, dt - (s+1)\int_0^T \int_D \partial_{Y_n}\nu\, \boldsymbol{\varphi}_{tt}\cdot\partial_{Y_n}^{s}\mathbf{u}\, d\mathbf{x}\, dt \\
&\quad + (s+1)\int_D \partial_{Y_n}\nu\left[\boldsymbol{\varphi}(0,\mathbf{x},Y)\cdot\partial_{Y_n}^{s}\mathbf{g}_2(\mathbf{x}) - \boldsymbol{\varphi}_t(0,\mathbf{x},Y)\cdot\partial_{Y_n}^{s}\mathbf{g}_1(\mathbf{x})\right] d\mathbf{x}. \qquad (32)
\end{aligned}
$$

Note that the last term in (32) is zero for $s \geq 1$. Therefore, (30) follows for $k = 0$.

General case $k \geq 1$**.** We assume that (30) holds for every $s \geq 0$ and $0 \leq k \leq K$ and show that

$$
\begin{aligned}
d_{Y_n}^{s+K+2}\mathcal{Q}(Y) &= C_{s,K+1}\int_0^T \int_D \nabla\partial_{Y_n}^{K+1}\boldsymbol{\varphi} : \tilde{\boldsymbol{\sigma}}(\partial_{Y_n}^{s}\mathbf{u})\, d\mathbf{x}\, dt \\
&\quad + C_{s,K+1}\int_0^T \int_D \partial_{Y_n}\nu\, \partial_{Y_n}^{K+1}\boldsymbol{\varphi}_{tt}\cdot\partial_{Y_n}^{s}\mathbf{u}\, d\mathbf{x}\, dt \\
&\quad + C_{s,K+1}\int_D \partial_{Y_n}\nu\left[\partial_{Y_n}^{K+1}\boldsymbol{\varphi}(0,\mathbf{x},Y)\cdot\partial_{Y_n}^{s}\mathbf{g}_2(\mathbf{x}) - \partial_{Y_n}^{K+1}\boldsymbol{\varphi}_t(0,\mathbf{x},Y)\cdot\partial_{Y_n}^{s}\mathbf{g}_1(\mathbf{x})\right] d\mathbf{x}. \qquad (33)
\end{aligned}
$$

We first differentiate the induction hypothesis (30) for $k = K$ with respect to Y_n and get

$$
\begin{aligned}
d_{Y_n}^{s+K+2}\mathcal{Q}(Y) &= C_{s,K}\int_0^T \int_D \nabla\partial_{Y_n}^{K+1}\boldsymbol{\varphi} : \tilde{\boldsymbol{\sigma}}(\partial_{Y_n}^{s}\mathbf{u})\, d\mathbf{x}\, dt + C_{s,K}\int_0^T \int_D \nabla\partial_{Y_n}^{K}\boldsymbol{\varphi} : \tilde{\boldsymbol{\sigma}}(\partial_{Y_n}^{s+1}\mathbf{u})\, d\mathbf{x}\, dt \\
&\quad + C_{s,K}\int_0^T \int_D \partial_{Y_n}\nu\, \partial_{Y_n}^{K+1}\boldsymbol{\varphi}_{tt}\cdot\partial_{Y_n}^{s}\mathbf{u}\, d\mathbf{x}\, dt + C_{s,K}\int_0^T \int_D \partial_{Y_n}\nu\, \partial_{Y_n}^{K}\boldsymbol{\varphi}_{tt}\cdot\partial_{Y_n}^{s+1}\mathbf{u}\, d\mathbf{x}\, dt \\
&\quad + C_{s,K}\int_D \partial_{Y_n}\nu\left[\partial_{Y_n}^{K+1}\boldsymbol{\varphi}(0,\mathbf{x},Y)\cdot\partial_{Y_n}^{s}\mathbf{g}_2(\mathbf{x}) - \partial_{Y_n}^{K+1}\boldsymbol{\varphi}_t(0,\mathbf{x},Y)\cdot\partial_{Y_n}^{s}\mathbf{g}_1(\mathbf{x})\right] d\mathbf{x}. \qquad (34)
\end{aligned}
$$

Next, we note that the hypothesis holds also for $s+1$ and $k=K$,

$$d_{Y_n}^{s+K+2}\mathcal{Q}(Y) = C_{s+1,K}\int_0^T\int_D \nabla\partial_{Y_n}^K\boldsymbol{\varphi} : \tilde{\boldsymbol{\sigma}}(\partial_{Y_n}^{s+1}\mathbf{u})\,d\mathbf{x}\,dt + C_{s+1,K}\int_0^T\int_D \partial_{Y_n}\nu\,\partial_{Y_n}^K\boldsymbol{\varphi}_{tt}\cdot\partial_{Y_n}^{s+1}\mathbf{u}\,d\mathbf{x}\,dt. \tag{35}$$

Using (34) and (35), we can eliminate the terms involving $\partial_{Y_n}^{s+1}u$ and obtain (33). This completes the proof. □

As a corollary of Theorem 4.4, we can write:

Corollary 4.1 *With the assumptions of Theorem 4.4, we have* $d_{Y_n}^{s+k+1}\mathcal{Q}\in L^\infty(\Gamma)$.

Similarly, we can study the mixed Y-derivatives of $\mathcal{Q}$.

Theorem 4.5 *Let* $k,s\in\mathbb{N}$ *be two non-negative integers. Moreover, assume that* $\boldsymbol{\phi}\in\mathbf{H}^k(D)$. *Then, under the assumptions* (16)-(17) *and with random coefficients satisfying* (4)-(7), *we have* $d_Y^{\mathbf{m}}\mathcal{Q}\in L^\infty(\Gamma)$ *for a multi-index* $\mathbf{m}\in\mathbb{N}^N$ *with* $|\mathbf{m}|=s+k+1$. *In particular, when* $\boldsymbol{\phi}\in\mathbf{C}^\infty(D)$, *then* $\mathcal{Q}\in C^\infty(\Gamma)$.

Proof. The proof is similar to the proof of Theorem 4.4 by an easy modification of the technique used in [26] for the representation of mixed derivatives. □

4.2.2 Filtered solutions

In seismology and petroleum and gas industry, the simulated seismic data are often post-processed. One typical type of post-processing is filtering the data. For instance, a low-pass filter (LPF) is used in order to isolate and remove the high-frequency noise in the solution. In fact, the source time functions (see Section 6.2) trigger high frequency motions which are not resolvable on the mesh. The simulated solutions are therefore low-pass filtered and the high frequency errors are cut off. This is done by convolving the solution $u(t,\mathbf{x})$ with some smooth Kernels known as transfer functions. Two frequently used filters are Gaussian and Butterworth LPFs whose transfer functions read

$$K_\sigma^G(\mathbf{x}) = \frac{1}{2\,\pi\,\sigma^2}\,e^{-\frac{|\mathbf{x}|^2}{2\,\sigma^2}}, \qquad K_{n,r}^B(\mathbf{x}) = \frac{1}{\prod_{i=1}^d\left(1+(x_i/r)^{2\,n}\right)}, \tag{36}$$

respectively. In a Gaussian LPF, the standard deviation σ is inversely proportional to the maximum frequency that is allowed to pass. In a Butterworth LPF, the order n controls the sharpness of the cutoff, and r represents the frequency where the cut-off occurs. Fig. 1a shows the one-dimensional normalized Gaussian transfer function $2\,\pi\,\sigma^2\,K_\sigma^G(x)$ for different values of σ, and Fig. 1b shows the one-dimensional Butterworth transfer function $K_{n,r}^B(x)$ with $r=3$ and for different values of n. The value of r corresponds to the point where the Butterworth transfer function has value 1/2.

The filtered solution is then given by

$$\mathbf{u}^f(t,\mathbf{x}) = (\mathbf{u}\star K_\sigma)(t,\mathbf{x}) = \int_D K(\mathbf{x}-\tilde{\mathbf{x}})\,\mathbf{u}(t,\tilde{\mathbf{x}})\,d\tilde{\mathbf{x}}, \tag{37}$$

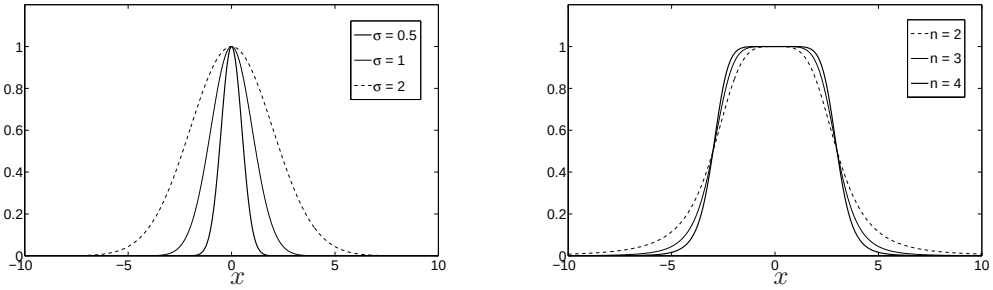

(a) $2\,\pi\,\sigma^2\,K_\sigma^G$ (b) $K_{n,3}^B$

Figure 1: Transform functions for the one-dimensional Gaussian and Butterworth LPFs.

with the Kernel K given by either a Gaussian or a Butterworth transfer function in (36). We note that the filtered solution (37) is of a type similar to the quantity of interest (27). However, the main difference here is the boundary effects due to the convolution. Therefore, following the results of Sections 4.1 and 4.2.1, in the presence of a compactly supported smooth kernel $K \in C_0^\infty(D)$ as mollifier, the quantity (37) has high Y-regularity in the regions away enough from the boundary ∂D for which the support of $K(\mathbf{x} - \tilde{\mathbf{x}})$ does not cross the boundary ∂D. Although the smooth kernels given by (36) are not compactly supported, as we notice in Fig. 1, for small values of σ in the Gaussian filter and for large values of n and small values of r in the Butterworth filter, the kernels may be considered as *essentially* compactly supported. Hence, for such Gausian and Butterworth LPFs, the filtered solution in points away from the boundary behaves as a quantity of interest with high Y-regularity. We refer to the test 2 in Section 6 for a numerical verification of high Y-regularity of a smoothed solution by a Gaussian filter.

5 Stochastic collocation

The stochastic collocation method consists of three main steps. First, the problem (1) is discretized in space and time, using a deterministic numerical method, such as the finite element or the finite difference method. The obtained semi-discrete problem is then collocated in a set of η collocation points $\{Y^{(k)}\}_{k=1}^{\eta} \in \Gamma$ to compute the approximate solutions $u_h(t, \mathbf{x}, Y^{(k)})$. Finally, a global polynomial approximation $u_{h,p}$ is built upon those evaluations

$$u_{h,p}(t, \mathbf{x}, Y) = \sum_{k=1}^{\eta} u_h(t, \mathbf{x}, Y^{(k)})\, L_k(Y),$$

for suitable multivariate polynomials $\{L_k\}_{k=1}^{\eta}$ such as Lagrange polynomials. Here, h and p represent the discretization mesh size and the polynomial degree, respectively. For more details we refer to [2, 44].

A key point in the stochastic collocation method is the choice of the set of collocation points $\{Y^{(k)}\}$, i.e. the type of computational grid in the N-dimensional stochastic space. A full tensor grid, based on cartesian product of mono-dimensional grids, can only be used when the number of stochastic dimensions N is small, since the computational cost grows exponentially fast with N (*curse of dimensionality*). To clarify this, let $\ell \in \mathbb{N}$ be a non-negative integer, called the *level*. Moreover, for a given index $j \in \mathbb{N}$, let $p(j)$ be a polynomial degree. Typical choices of the function p include

$$p(j) = j, \tag{38}$$

and

$$p(j) = 2^j \text{ for } j > 0, \qquad p(0) = 0. \tag{39}$$

In the full tensor grid, in each direction we take all polynomials of degree at most $p(\ell)$, and therefore $(p(\ell)+1)^N$ grid points are needed.

Alternatively, sparse grids can reduce the curse of dimensionality. They were originally introduced by Smolyak for high dimensional quadrature and interpolation computations [34]. In the following we will briefly review and generalize the sparse grid construction.

Let $\mathbf{j} \in \mathbb{Z}_+^N$ be a multi-index containing non-negative integers. For a non-negative index j_n in $\mathbf{j}$, we introduce a sequence of one-dimensional polynomial interpolant operators $\mathcal{U}^{j_n} : C^0(\Gamma_n) \to \mathbb{P}_{p(j_n)}(\Gamma_n)$ on $p(j_n)+1$ suitable knots. With $\mathcal{U}^{-1} = 0$, we define the detail operator

$$\Delta^{j_n} := \mathcal{U}^{j_n} - \mathcal{U}^{j_n - 1}.$$

Finally, introducing a sequence of index sets $\mathcal{I}(\ell) \subset \mathbb{Z}_+^N$, the sparse grid approximation of $u : \Gamma \to V$ at level ℓ reads

$$u_\ell(., Y) = \mathcal{S}_{\mathcal{I}(\ell),N}[u](., Y) = \sum_{\mathbf{j} \in \mathcal{I}(\ell)} \bigotimes_{n=1}^{N} \Delta^{j_n}[u](., Y). \tag{40}$$

The statistical moments of the solution or some given quantities of interest are computed by the Gauss quadrature formula corresponding to each interplant operator for approximating integrals [26]. We note that $V = \mathbf{C}^0((0,T); \mathbf{H}^{s+1}(D))$ as in (18), and the regularity of the mapping $\Gamma \to V$ is given by (22). Furthermore, in order for the sum (40) to have some telescopic properties, which are desirable, we impose an additional admissibility condition on the set $\mathcal{I}$ [10]. An index set $\mathcal{I}$ is said to be *admissible* if $\forall \mathbf{j} \in \mathcal{I}$,

$$\mathbf{j} - \mathbf{e}_n \in \mathcal{I} \quad \text{for } 1 \le n \le N, \quad j_n \ge 1,$$

holds. Here, $\mathbf{e}_n$ is the n-th canonical unit vector.

To fully characterize the sparse approximation operator in (40), we need to provide the following:

- A level $\ell \in \mathbb{N}$ and a function $p(j)$ representing the relation between an index j and the number of points in the corresponding one-dimensional polynomial interpolation formula $\mathcal{U}^j$.

- A sequence of sets $\mathcal{I}(\ell)$.
- The family of points to be used, such as Gauss or Clenshaw-Curtis abscissae, [39].

Typical examples of index sets include

1. Full tensor grid: $\mathcal{I}(\ell) = \{\mathbf{j} : \max_n j_n \leq \ell\}$.
2. Total degree sparse grid: $\mathcal{I}(\ell) = \{\mathbf{j} : \sum_{n=1}^{N} j_n \leq \ell\}$ with $p(j) = j$.
3. Hyperbolic cross sparse grid: $\mathcal{I}(\ell) = \{\mathbf{j} : \prod_{n=1}^{N}(j_n + 1) \leq \ell + 1\}$ with $p(j) = j$.

We now briefly motivate the construction of the hyperbolic cross sparse grid based on a simple optimality argument. A rigorous optimal sparse grid construction will be addressed elsewhere.

Let the error associated to a sparse grid be

$$E_{\mathcal{S}} = ||u - \mathcal{S}_{\mathcal{I}(\ell),N}[u]||_{V \otimes L^2_\rho(\Gamma)},$$

and the work $W_{\mathcal{S}}$ be the number of collocation points in the grid. We aim at finding the optimal set of indices that minimizes the error with a total work smaller than or equal to a given maximum work. For this purpose, we introduce the error and work contribution of a multi-index $\mathbf{j}$ as $E_{\mathbf{j}}$ and $W_{\mathbf{j}}$, respectively. We then define the profit of an index as

$$P_{\mathbf{j}} = \frac{E_{\mathbf{j}}}{W_{\mathbf{j}}},$$

and choose the optimal set including the most profitable indices: $\mathcal{I}^*(\epsilon) = \{\mathbf{j} \in \mathbb{N}^N : P_{\mathbf{j}} \geq \epsilon\}$, with a given positive threshold $\epsilon > 0$ [3, 13, 4, 10].

Deriving a rigorous bound for the error is not easy. We denote the norm of each detail from (40) by

$$E_{\mathbf{j}} = ||\mathcal{S}_{\mathcal{I}(\ell),N}[u] - \mathcal{S}_{\mathcal{I}(\ell)\setminus\mathbf{j},N}[u]|| = ||\bigotimes_{n=1}^{N} \Delta^{j_n}[u]||, \tag{41}$$

where $\mathcal{I}(\ell)$ is any admissible index set containing $\mathbf{j}$ such that $\mathcal{I}(\ell) \setminus \mathbf{j}$ is still admissible. For a function u with $s \geq 1$ bounded mixed Y-derivatives, we have [26]

$$E_{\mathbf{j}} \leq C \prod_{n=1}^{N} p(j_n)^{-s},$$

where C depends on s, N, and the size of all mixed Y-derivatives of u, but is independent of p and ℓ. We simplify the bound by setting $C \equiv 1$. The work, for non-nested grids, can be defined as $W_{\mathbf{j}} = W_{\mathcal{I}(\ell)} - W_{\mathcal{I}(\ell)\setminus\mathbf{j}}$ and can be bounded by

$$W_{\mathbf{j}} \leq \prod_{n=1}^{N} (p(j_n) + 1). \tag{42}$$

We notice that the error contribution (41) of a multi-index $\mathbf{j}$ is always independent of the set $\mathcal{I}(\ell)$ to which the multi-index is added. However, the work associated to a multi-index $\mathbf{j}$ depends, in general, on the set $\mathcal{I}(\ell)$, except in the case of nested grids (see Remark 5.1). Therefore, for non-nested grids, (42) is only an upper bound of the work, independent of $\mathcal{I}(\ell)$.

We can now estimate the profit of each multi-index and build an optimal set

$$\mathcal{I}^*(\epsilon) = \{\mathbf{j} \in \mathbb{N}^N : \frac{\prod_{n=1}^N p(j_n)^{-s}}{\prod_{n=1}^N (p(j_n)+1)} \geq \epsilon\}.$$

Equivalently, for $\ell = 0, 1, \ldots$ and large $p(j_n)$, we have

$$\mathcal{I}^*(\ell) = \{\mathbf{j} \in \mathbb{N}^N : \sum_{n=1}^N \log(p(j_n)+1) \leq \ell\},$$

which is a hyperbolic cross grid. We refer to the numerical test 2 in Section 6 for a numerical verification of the advantage of using hyperbolic cross grids over total degree grids.

Remark 5.1 *In the case of using Smolyak-type grids with nested points* (39)*, we can obtain a sharper bound for the work:*

$$W_{\mathbf{j}} = \prod_{n=1}^N (p(j_n) + 1 - p(j_n - 1) - 1) = \prod_{n=1}^N 2^{j_n - 1}.$$

In this case we will also get

$$E_{\mathbf{j}} \leq C \prod_{n=1}^N p(j_n)^{-s} = C \prod_{n=1}^N 2^{-j_n\, s} = C\, 2^{-s \sum_{n=1}^N j_n},$$

and therefore the set $\mathcal{I}^*(\ell) = \{\mathbf{j} \in \mathbb{N}^N : \sum_{n=1}^N j_n \leq \ell\}$ *is optimal among nested grids for which* $p(j) = 2^j$*. Notice that this choice corresponds to the classical Smolyak construction.*

6 Numerical experiments

In this section, we consider the IBVP (1) in a two dimensional rectangular domain $D = [-1, 1] \times [-2, 0]$. We numerically simulate the problem by the stochastic collocation method and study the convergence of the statistical moments of the solution $\mathbf{u}$, the linear quantity of interest (27), and the filtered solution (37) using a Gaussian low-pass filter.

The deterministic solver employs an explicit, second order accurate finite difference method which discretizes the PDEs in its second order form [27]. We note that an alternative approach is to first rewrite the second order system (1) as a larger system

of first order equations and then discretize the new system. This approach however has the disadvantage of introducing auxiliary variables with their associated constraints and boundary conditions. This in turn reduces computational efficiency and accuracy [16, 18]. In the stochastic space, we use collocation on a variety of sparse grids based on Gauss abscissas.

We perform two numerical tests. In the first test, we consider zero initial data and a non-zero force term. In the second test, we simulate a simplified earthquake problem with slip on an extended fault surface. For both tests, we consider zero initial data $\mathbf{g}_1 = \mathbf{g}_2 = \mathbf{0}$ and apply a stress-free boundary condition (1c) with $\mathbf{h} = \mathbf{0}$ at $z = 0$ and Clayton-Engquist non-reflecting boundary conditions (12) at the other edges. We study the convergence rate of the low-regular solution and high-regular quantities of interest.

6.1 Numerical test 1

In the first test, we consider a time-dependent force term $\mathbf{f} = (f_1, f_2)^\top$ with $f_1 = f_2 = -\mathcal{S}(t)\, F(x, z)$, where

$$\mathcal{S}(t) = \begin{cases} 1, & t \in [0, 0.1) \cup [0.2, 0.4), \\ 0.5, & otherwise, \end{cases}$$

and

$$F(x, z) = \begin{cases} 500\,(0.2 - |x|), & \mathbf{x} \in C \text{ and } |z + 1| \le |x|, \\ 500\,(0.2 - |z + 1|), & \mathbf{x} \in C \text{ and } |z + 1| > |x|, \\ 0, & otherwise, \end{cases}$$

and $C = [-0.2, 0.2] \times [-1.2, -0.8]$, see Fig. 2. Note that, with this choice, we have $\mathbf{f} \in \mathbf{L}^2((0, T); \mathbf{H}^1(D))$.

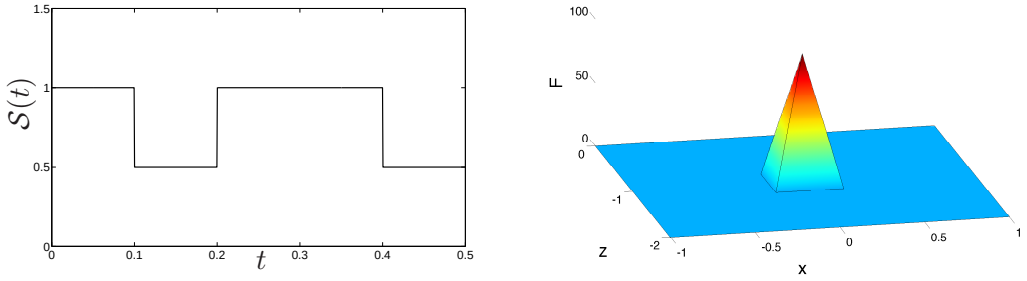

(a) $\mathcal{S} \in L^2(0, T)$ (b) $F \in H^1(D)$

Figure 2: Test 1. The force term $\mathbf{f} = (f_1, f_2)^\top$ given by $f_1 = f_2 = -\mathcal{S}(t)\, F(x, z)$.

We consider the following $\mathbf{x}$-smooth random coefficients

$$\begin{aligned}\nu(\mathbf{x}, Y) &= 2.6,\\ \mu(\mathbf{x}, Y) &= 2.5 + \cos\frac{4\,\pi\,z\,Y_1}{L_z} + \sin\frac{6\,\pi\,z\,Y_2}{L_z},\\ \lambda(\mathbf{x}, Y) &= 2\,\mu,\end{aligned}$$

with two independent and uniformly distributed random variables $Y_n \sim \mathcal{U}(0.1, 0.5)$, $n = 1, 2$. Note that the above coefficients satisfy the assumptions (4)-(7).

We employ the collocation method on a hyperbolic cross sparse grid. We use a time step-size $\Delta t = \Delta x/4$ which guarantees the stability of the deterministic numerical solver. We study the convergence rate of the sparse grid collocation for two different choices of spatial grid-lenghts $\Delta x = \Delta z = 0.05, 0.025$. For each grid-length $\Delta x = h$, we consider different levels $\ell \geq 1$ and compute the L^2-norm of error in the expected value of the solution on a part of the domain $D_0 \subset D$ at a fixed time $t = T$ by

$$\varepsilon_{\mathbf{u}} := \Big(\int_{D_0} \Big|\mathbb{E}\left[\mathbf{u}_{h,\ell}\right](T, \mathbf{x}) - \mathbb{E}\left[\mathbf{u}_{h,\ell_{\text{ref}}}\right](T, \mathbf{x})\Big|^2 \, d\mathbf{x}\Big)^{1/2}. \tag{43}$$

Here, the reference solution $\mathbf{u}_{h,\ell_{\text{ref}}}$ is computed with a high level $\ell_{\text{ref}} > \ell$ for the same $\Delta x = h$. In this test, we choose $D_0 = D$ and $T = 0.5$.

We also compute the error in the expected value of the quantity of interest (27) at $T = 0.5$ by

$$\varepsilon_{\mathcal{Q}} := \Big|\mathbb{E}\left[\mathcal{Q}[\mathbf{u}_{h,\ell}]\right] - \mathbb{E}\left[\mathcal{Q}[\mathbf{u}_{h,\ell_{\text{ref}}}]\right]\Big|,$$

with a smooth mollifier $\boldsymbol{\phi} = (\phi_1, \phi_2)^\top \in \mathbf{C}_0^\infty(D)$, where

$$\phi_1(x, z) = \phi_2(x, z) = \begin{cases} 50\,\exp\Big(\frac{0.32}{(x-0.4)^2-0.16} + \frac{0.32}{(z+0.4)^2-0.16}\Big), & \mathbf{x} \in D_\phi \setminus \partial D_\phi,\\ 0, & otherwise,\end{cases}$$

with the support $D_\phi = [0, 0.8] \times [-0.8, 0] \subset D$.

We note that since $\mathbf{f} \in \mathbf{L}^2(0, T; \mathbf{H}^1(D))$, by Theorem 4.2 for $s = 1$, we will have

$$\partial_{Y_n}^k \mathbf{u} \in \mathbf{L}^\infty(\Gamma; \mathbf{C}^0([0, T]; \mathbf{H}^{2-k}(D))), \qquad 0 \leq k \leq 2.$$

Therefore, the solution has only two bounded Y-derivatives in $\mathbf{C}^0([0, T]; \mathbf{L}^2(D))$ and one bounded mixed Y-derivatives. Consequently, we expect a slow rate of error convergence for $\varepsilon_{\mathbf{u}}$. On the other hand, due to high Y-regularity of the quantity of interest, we expect a fast convergence rate for $\varepsilon_{\mathcal{Q}}$. Fig. 3 shows these two quantities versus the number of collocation points $\eta(\ell)$. We observe a slow convergence of order $\mathcal{O}(\eta^{-1})$ for $\varepsilon_{\mathbf{u}}$ and a faster convergence for $\varepsilon_{\mathcal{Q}}$, as expected. We also notice that for large values of $h\,\eta$, we observe exponential decay in the error $\varepsilon_{\mathbf{u}}$, and as h decreases, more collocation points are needed to maintain a fixed accuracy. In fact, as showed in [26], using the inverse inequality, we can show that the semi-discrete solution $\mathbf{u}_h$ can analytically be extended to a region in the complex plane with a radius proportional to h. Therefore, in building an approximate solution $\mathbf{u}_{h,\ell}$ to $\mathbf{u}_h$, we will observe a fast exponential

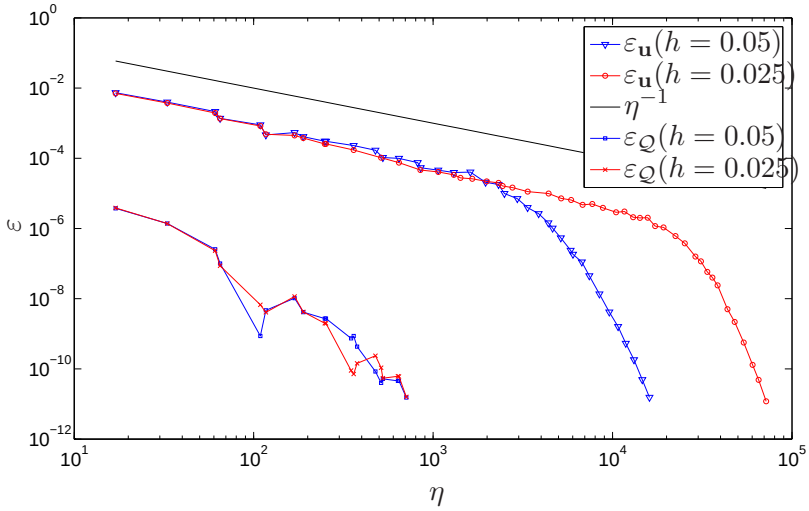

Figure 3: Test 1. The L^2-norm of error in the expected value of the solution $\varepsilon_{\mathbf{u}}$ and the error in the expected value of the quantity of interest $\varepsilon_{\mathcal{Q}}$ at time $T = 0.5$ versus the number of collocation points $\eta(\ell)$. The solution has only two bounded Y-derivatives and one bounded mixed Y-derivative. However, the quantity of interest has bounded mixed Y-derivatives of any order and possesses high Y-regularity.

decay in the error when the product $h\,\ell$ is large. Consequently, with a fixed h, the error convergence is slow (algebraic) for a small ℓ and fast (exponential) for a large ℓ. Moreover, the rate of convergence deteriorates as h gets smaller.

6.2 Numerical test 2

In the second test, we simulate a simplified earthquake problem with slip on an extended fault surface. We consider a two-dimensional problem which is similar to the three-dimensional problem LOH.2 defined by the Pacific Earthquake Engineering Center [7].

In seismic wave propagation due to earthquakes and explosions, the source term is often composed of point sources (point moments) distributed over a fault surface,

$$\mathbf{f}(t,\mathbf{x}) = \sum_r \mathbf{f}_r^{(M)}(t,\mathbf{x}), \qquad \mathbf{f}_r^{(M)}(t,\mathbf{x}) = \mathcal{S}_r(t)\,\mathbf{M}_r\,\nabla\delta(\mathbf{x}-\mathbf{x}_r), \tag{44}$$

where $\mathcal{S}_r$ is the source time function, $\mathbf{M}_r$ is a constant symmetric matrix, and $\nabla\delta$ is the gradient of the Dirac distribution. Each term in (44) is applied at a location $\mathbf{x}_r = (x_r, z_r)$ which is independent of the grid $\mathbf{x}_{i,j}$. Based on the analysis of [42, 38], it is possible to derive regularized approximations of the Dirac distribution and its gradient, which result in point-wise convergence of the solution away from the sources. The derivation of approximations of the Dirac distribution and its gradient is based

on the following properties,

$$\int \phi(\mathbf{x})\,\delta(\mathbf{x}-\mathbf{x}_r)\,d\mathbf{x} = \phi(\mathbf{x}_r), \qquad \int \phi(\mathbf{x})\,\partial_x\delta(\mathbf{x}-\mathbf{x}_r)\,d\mathbf{x} = -\partial_x\phi(\mathbf{x}_r),$$

which holds for any smooth function ϕ. In one-dimension with a uniform grid x_k with grid size h, the integrals are replaced by a discrete scalar product $(p,q)_{1,h} := h\sum p_i\,q_i$. Cubic approximations of the Dirac distribution and its gradient are then obtained when the integral conditions are satisfied with ϕ being polynomials of degree three. Let $x_k \le x_r < x_{k+1}$ and $\alpha = (x_r - x_k)/h$. Then a third order discretization of $\delta(x-x_r)$ is given by

$$\begin{aligned}
\delta_{k-1} &= \frac{1}{h}\,(-\alpha/3 + \alpha^2/2 - \alpha^3/6),\\
\delta_{k} &= \frac{1}{h}\,(1 - \alpha/2 - \alpha^2 + \alpha^3/2),\\
\delta_{k+1} &= \frac{1}{h}\,(\alpha + \alpha^2/2 - \alpha^3/2),\\
\delta_{k+2} &= \frac{1}{h}\,(-\alpha/6 + \alpha^3/6),\\
\delta_{j} &= 0, \quad j \notin \{k-1, k, k+1, k+2\}.
\end{aligned}$$

Similarly, a third order discretization of $\delta'(x-x_r)$ is given by

$$\begin{aligned}
\delta'_{k-1} &= \frac{1}{h^2}\,(1/3 - \alpha + \alpha^2/2),\\
\delta'_{k} &= \frac{1}{h^2}\,(1/2 + 2\,\alpha - 3\,\alpha^2/2),\\
\delta'_{k+1} &= \frac{1}{h^2}\,(-1 - \alpha + 3\,\alpha^2/2),\\
\delta'_{k+2} &= \frac{1}{h^2}\,(1/6 - \alpha^2/2),\\
\delta'_{j} &= 0, \quad j \notin \{k-1, k, k+1, k+2\}.
\end{aligned}$$

For a two-dimensional problem, for instance, we then use

$$\delta(\mathbf{x}-\mathbf{x}_r) \approx \delta(x-x_r)\,\delta(z-z_r),$$

and

$$\nabla\delta(\mathbf{x}-\mathbf{x}_r) \approx \begin{pmatrix} \delta'(x-x_r)\,\delta(z-z_r) \\ \delta(x-x_r)\,\delta'(z-z_r) \end{pmatrix}.$$

Using this representation, we obtain overall second order convergence of the solution away from the singularity at $\mathbf{x}_r$ [32].

We model the slip on the extended fault by distributing point moment sources on a regular grid with size $\Delta s = 0.1$ (which is independent of the computational grid size

$h = \Delta x = \Delta z$) over the fault surface given by $-0.3 \le x \le 0.1$, $-1.2 \le z \le -0.8$. The moment tensor in each source term is

$$\mathbf{M}_r = 7.5\,(\Delta s)^2 \begin{pmatrix} 1 & 0 \\ 0 & 0 \end{pmatrix}.$$

The earthquake starts at the hypocenter $\mathbf{x}_H = (-0.1, -1)$, and the rupture propagates along the fault surface with a uniform rupture velocity $c_{\rm rup} = 1.7$. We use the source time function

$$\mathcal{S}_r(t) = \begin{cases} 0, & t < R_r/c_{\rm rup}, \\ 1 - \left(1 + \frac{t - R_r/c_{\rm rup}}{\tau}\right) e^{\frac{-(t-R_r/c_{\rm rup})}{\tau}}, & t \ge R_r/c_{\rm rup}, \end{cases}$$

where $\tau = 0.1$ is related to the rise time of the slip, and $R_r = |\mathbf{x}_r - \mathbf{x}_H|$. See Fig. 4. Based on this time function, each point source gets activated as soon as the rupture started from the hypocenter reaches the point source. We note that the size of the rise time τ is related to the frequency of the seismic waves it generates: the smaller the rise time, the higher the frequency.

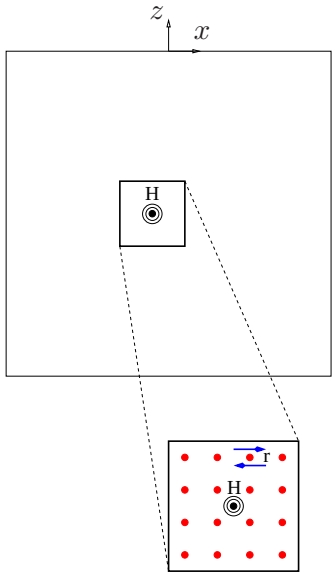

Figure 4: Test2. The computational domain and fault surface. The tick rectangle shows the fault surface, where the slip starts at the hypocenter indicated by concentric circles. Point moment sources are distributed on a regular grid on the fault surface.

We consider the following $\mathbf{x}$-smooth random coefficients of form (8)

$$\nu(\mathbf{x}, Y) = 2.6,$$

$$\mu(\mathbf{x}, Y) = 1.5 + Y_1 + 0.15 \sum_{k=1}^{2} (Y_{2\,k} \cos \frac{2\,k\,\pi\,z}{L_z} + Y_{2\,k+1} \sin \frac{2\,k\,\pi\,z}{L_z}),$$

$$\lambda(\mathbf{x}, Y) = 2\,\mu(\mathbf{x}, Y),$$

where $Y_n \sim \mathcal{U}(0.1, 0.5)$, $n = 1, 2, \ldots, 5$, are five independent and uniformly distributed random variables.

We first employ the collocation method on a total degree sparse grid. We use a time step-size $\Delta t = \Delta x/4$ which guarantees the stability of the deterministic numerical solver. We compute the L^2-norm of error in the expected value of the solution (43) on $D_0 = [-1, 1] \times [-0.8, 0]$ at $T = 1$. We also compute the L^2-norm of error in the expected value of the filtered solution (37) at a fixed time $t = T$ by

$$\varepsilon_{\mathbf{u}^f} := \Big(\int_{D_f} \Big| \mathbb{E}\left[\mathbf{u}^f_{h,\ell}\right](T, \mathbf{x}) - \mathbb{E}\left[\mathbf{u}^f_{h,\ell_{\text{ref}}}\right](T, \mathbf{x}) \Big|^2 d\mathbf{x} \Big)^{1/2}, \tag{45}$$

over a window $D_f = [0.1, 0.2] \times [-1.1, -.9] \subset D$ away from the boundary ∂D. Here, the reference solution $\mathbf{u}^f_{h,\ell_{\text{ref}}}$ is again computed with a high level $\ell_{\text{ref}} > \ell$ on the same grid with $\Delta x = h$.

Fig. 5 shows the L^2-norm of error in the expected value of the solution $\varepsilon_{\mathbf{u}}$ and the error in the expected value of the filtered solution $\varepsilon_{\mathbf{u}^f}$ using a Gaussian Kernel K^G_σ in (36) with $\sigma = 2$ at $T = 1$ versus the number of collocation points $\eta(\ell)$. For

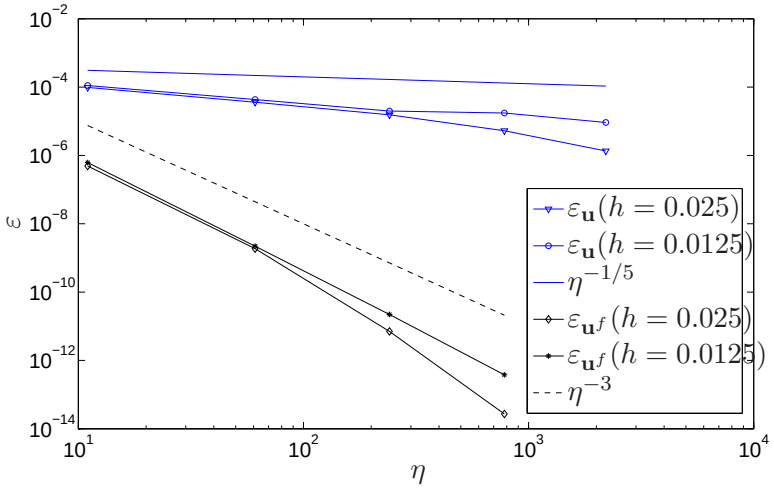

Figure 5: Test 2. The L^2-norm of error in the expected value of the solution $\varepsilon_{\mathbf{u}}$ and the error in the expected value of the filtered solution $\varepsilon_{\mathbf{u}^f}$ at $T = 1$ versus the number of collocation points $\eta(\ell)$. The solution has no bounded Y-derivatives. However, the filtered solution behaves has a quantity with high Y-regularity.

the solution, there is no bounded Y-derivatives due to the presence of $\nabla\delta$ in the force term (44). We observe a slow convergence of order $\mathcal{O}(\eta^{-\delta})$ with $0 < \delta < 1/5$. On the other hand, for the filtered solution, we observe a fast convergence rate of order about $\mathcal{O}(\eta^{-3})$, which verifies that the filtered solution behaves as a quantity with high Y-regularity, as discussed in Section 4.2.2.

Next, we compare the performance of the collocation method on two different sparse grids; the total degree grid and the hyperbolic cross grid. Fig 6 shows the L^2-norm of

error in the expected value of the solution at $T = 1$ versus the number of collocation points $\eta(\ell)$ obtained by two different sparse grids. We clearly observe the advantage of using hyperbolic cross grids over total degree grids as predicted in Section 5.

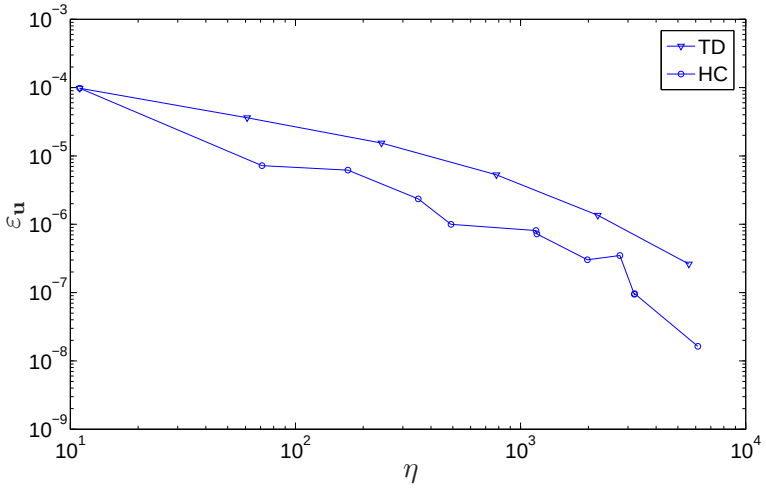

Figure 6: Test 2. The L^2-norm of error in the expected value of the solution $\varepsilon_{\mathbf{u}}$ at time $T = 1$ versus the number of collocation points $\eta(\ell)$ computed on the total degree (TD) and the hyperbolic cross (HC) sparse grids.

7 Conclusions

We have analyzed the stochastic initial-boundary value problem for the elastic wave equation with random coefficients and deterministic data. We consider a random heterogeneous medium with time-independent and smooth material properties. We also assume that the wave length is not very small compared to the overall size of the domain and is comparable to the scale of the variations in the medium. We have studied the well-posedness and stochastic regularity of the problem by employing the energy method. We have also proposed a stochastic collocation method for computing statistical moments of the solution or some given quantities of interest and studied the convergence rate of the error.

The main result is that the stochastic regularity of the solution or the quantity of interest is closely related to the regularity of the deterministic data in the physical space and the type of the quantity of interest. We demonstrate that high stochastic regularity is possible in two cases: for the elastic wave solutions with high regular data; and for some high regular physical quantities of interest even in the presence of low regular data. For such problems, a fast spectral convergence is therefore possible when a stochastic collocation method is employed. The numerical examples presented in the paper are shown to be consistent with the analytical results and show that the

stochastic collocation method are a valid alternative to the more traditional Monte Carlo method for problems with high stochastic regularity.

Acknowledgements

The authors would like to recognize the support of the PECOS center at ICES, University of Texas at Austin (Project Number 024550, Center for Predictive Computational Science). Support from the VR project "Effektiva numeriska metoder för stokastiska differentialekvationer med tillämpningar" and King Abdullah University of Science and Technology (KAUST) AEA project "Bayesian earthquake source validation for ground motion simulation" is also acknowledged. The third author is a member of the KAUST SRI Center for Uncertainty Quantification in Computational Science and Engineering. The second author has been supported by the Italian grant FIRB-IDEAS (Project n. RBID08223Z) "Advanced numerical techniques for uncertainty quantification in engineering and life science problems".

References

[1] I. Babuska, R. Tempone, and G. E. Zouraris. Solving elliptic boundary value problems with uncertain coefficients by the finite element method: the stochastic formulation. *Computer Methods in Applied Mechanics and Engineering*, 194:1251–1294, 2005.

[2] I. M. Babuska, F. Nobile, and R. Tempone. A stochastic collocation method for elliptic partial differential equations with random input data. *SIAM J. Numer. Anal.*, 45:1005–1034, 2007.

[3] J. Bäck, F. Nobile, L. Tamellini, and R. Tempone. On the optimal polynomial approximation of stochastic PDEs by Galerkin and collocation methods. *Math. Mod. Methods Appl. Sci.*, 22, 2012.

[4] H.-J. Bungartz and M. Griebel. Sparse grids. *Acta Numer.*, 13:147–269, 2004.

[5] R. Clayton and B. Engquist. Absorbing boundary conditions for acoustic and elastic wave equations. *Bull. Seismol. Soc. Amer.*, 67:1529–1540, 1977.

[6] A. Cohen, R. DeVore, and Ch. Schwab. Convergence rates of best N-term Galerkin approximations for a class of elliptic sPDEs. *Foundations of Computational Mathematics*, 10:615–646, 2010.

[7] S. M. Day, J. Bielak, D. Dreger, S. Larsen, R. Graves, A. Ptarka, and K. B. Olsen. Tests of 3D elastodynamic codes: Lifelines program task 1A01. Technical report, Pacific Earthquake Engineering Center, 2001.

[8] L. C. Evans. *Partial Differential Equations*, volume 19 of *Graduate Studies in Mathematics*. American Mathematical Society, Providence, Rhode Island, 1998.

[9] G. S. Fishman. *Monte Carlo: Concepts, Algorithms, and Applications*. Springer-Verlag, New York, 1996.

[10] T. Gerstner and M. Griebel. Dimension-adaptive tensor-product quadrature. *Computing*, 71:65–87, 2003.

[11] R. G. Ghanem and P. D. Spanos. *Stochastic finite elements: A spectral approach*. Springer, New York, 1991.

[12] D. Gottlieb and D. Xiu. Galerkin method for wave equations with uncertain coefficients. *Commun. Comput. Phys.*, 3:505–518, 2008.

[13] M. Griebel and S. Knapek. Optimized general sparse grid approximation spaces for operator equations. *Math. Comp.*, 78:2223–2257, 2009.

[14] Lars Hörmander. *The Analysis of Linear Partial Differential Operators III, Pseudo-Differential Operators*. Classics in Mathematics, Springer, Berlin, 1994.

[15] H.-O. Kreiss. Initial boundary value problems for hyperbolic systems. *Commun. Pur. Appl. Math.*, 23:277–298, 1970.

[16] H.-O. Kreiss and O. E. Ortiz. Some mathematical and numerical questions connected with first and second order time-dependent systems of partial differential equations. *Lecture Notes in Physics*, 604:359–370, 2002.

[17] H.-O. Kreiss, O. E. Ortiz, and N. A. Petersson. Initial-boundary value problems for second order systems of partial differential equations. *Mathematical Modelling and Numerical Analysis*, 46:559–593, 2012.

[18] H.-O. Kreiss, N. A. Petersson, and J. Yström. Difference approximations for the second order wave equation. *SIAM J. Numer. Anal.*, 40:1940–1967, 2002.

[19] I. Lasiecka and R. Triggiani. Regularity theory of hyperbolic equations with nonhomogeneous Neumann boundary conditions. II. Ggeneral boundary data. *Journal of Differential Equations*, 94:112–164, 1991.

[20] I. Lasiecka and R. Triggiani. Recent advances in regularity of second-order hyperbolic mixed problems and applications. *In Dynamics Reported-Expositions in Dynamical Systems*, 3:23–104, 1994.

[21] G. Lin, C.-H. Su, and G. E. Karniadakis. Predicting shock dynamics in the presence of uncertainties. *J. Comput. Phys.*, 217:260–276, 2006.

[22] G. Lin, C.-H. Su, and G. E. Karniadakis. Stochastic modeling of random roughness in shock scattering problems: theory and simulations. *Comput. Methods Appl. Mech. Engrg.*, 197:3420–343, 2008.

[23] J. L. Lions and E. Magenes. *Non-homogeneous boundary value problems and applications I*. Springer- Verlag, Berlin, 1972.

[24] J. L. Lions and E. Magenes. *Non-homogeneous boundary value problems and applications II.* Springer- Verlag, Berlin, 1972.

[25] H. G. Matthies and A. Kees. Galerkin methods for linear and nonlinear elliptic stochastic partial differential equations. *Computer Methods in Applied Mechanics and Engineering*, 194:1295–1331, 2005.

[26] M. Motamed, F. Nobile, and R. Tempone. A stochastic collocation method for the second order wave equation with a discontinuous random speed. *Numer. Math.*, 2012. (to appear).

[27] S. Nilsson, N. A. Petersson, B. Sjögren, and H.-O. Kreiss. Stable difference approximations for the elastic wave equation in second order formulation. *SIAM J. Numer. Anal.*, 45:1902–1936, 2007.

[28] F. Nobile and R Tempone. Analysis and implementation issues for the numerical approximation of parabolic equations with random coefficients. *Int. J. Numer. Meth. Engng.*, 80:979–1006, 2009.

[29] F. Nobile, R. Tempone, and C. G. Webster. An anisotropic sparse grid stochastic collocation method for partial differential equations with random input data. *SIAM J. Numer. Anal.*, 46:2411–2442, 2008.

[30] F. Nobile, R. Tempone, and C. G. Webster. A sparse grid stochastic collocation method for partial differential equations with random input data. *SIAM J. Numer. Anal.*, 46:2309–2345, 2008.

[31] N. A. Petersson and B. Sjögreen. An energy absorbing far-field boundary condition for the elastic wave equation. *Commun. Comput. Phys.*, 6:483–508, 2009.

[32] N. A. Petersson and B. Sjögreen. Stable grid refinement and singular source discretization for seismic wave simulations. *Commun. Comput. Phys.*, 8:1074–111, 2010.

[33] G. Poette, B. Després, and D. Lucor. Uncertainty quantification for systems of conservation laws. *J. Comput. Phys.*, 228:2443–2467, 2009.

[34] S. A. Smolyak. Quadrature and interpolation formulas for tensor products of certain classes of functions. *Doklady Akademii Nauk SSSR*, 4:240–243, 1963.

[35] C. C. Stolk. *On the modeling and inversion of seismic data.* PhD thesis, Utrecht University, The Netherlands, 2000.

[36] T. Tang and T. Zhou. Convergence analysis for stochastic collocation methods to scalar hyperbolic equations with a random wave speed. *Commun. Comput. Phys.*, 8:226–248, 2010.

[37] R. A. Todor and C. Schwab. Convergence rates for sparse chaos approximations of elliptic problems with stochastic coefficients. *IMA J. Numer. Anal.*, 27:232–261, 2007.

[38] A.-K. Tornberg and B. Engquist. Numerical approximation of singular source terms in differential equations. *J. Comput. Phys.*, 200:462–488, 2004.

[39] L. N. Trefethen. Is gauss quadrature better than clenshawcurtis? *SIAM Rev.*, 50:67–87, 2008.

[40] J. Tryoen, O. Le Maitre, M. Ndjinga, and A. Ern. Intrusive projection methods with upwinding for uncertain nonlinear hyperbolic systems. *J. Comput. Phys*, 229:6485–6511, 2010.

[41] J. Tryoen, O. Le Maitre, M. Ndjinga, and A. Ern. Roe solver with entropy corrector for uncertain hyperbolic systems. . *Comput. Appl. Math.*, 235:491–506, 2010.

[42] J. Waldén. On the approximation of singular source terms in differential equations. *Numer. Methods Partial Differential Equations*, 15:503–520, 1999.

[43] X. Wang and G. E. Karniadakis. Long-term behavior of ploynomial chaos in stochastic flow simulations. *Computer Methods in Applied Mechanics and Engineering*, 195:5582–5596, 2006.

[44] D. Xiu and J. S. Hesthaven. High-order collocation methods for differential equations with random inputs. *SIAM J. Sci. Comput.*, 27:1118–1139, 2005.

[45] D. Xiu and G. E. Karniadakis. Modeling uncertainty in steady state diffusion problems via generalized polynomial chaos. *Computer Methods in Applied Mechanics and Engineering*, 191:4927–4948, 2002.

Recent publications :

MATHEMATICS INSTITUTE OF COMPUTATIONAL SCIENCE AND ENGINEERING
Section of Mathematics
Ecole Polytechnique Fédérale
CH-1015 Lausanne

19.2012 A. MANZONI, T. LASSILA, A. QUARTERONI, G. ROZZA:
A reduced-order strategy for solving inverse Bayesian shape identification problems in physiological flows

20.2012 J. BONNEMAIN. C. MALOSSI, M. LESINIGO, S. DEPARIS, A. QUARTERONI, L. VON SEGESSER:
Numerical simulation of left ventricular assist device implantations: comparing the ascending and the descending aorta cannulations

21.2012 A. ABDULLE, M. HUBER:
Discontinuous Galerkin finite element heterogeneous multiscale method for advection-diffusion problems with multiple scales

22.2012 R. ANDREEV, C. TOBLER:
Multilevel preconditioning and low rank tensor iteration for space-time simultaneous discretizations of parabolic PDES

23.2012 P. CHEN, A. QUARTERONI, G. ROZZA:
Stochastic optimal Robin boundary control problems of advection-dominated elliptic equations

24.2012 J. BECK, F. NOBILE, L. TAMELLINI, R. TEMPONE:
Convergence of quasi-optimal stochastic Galerkin methods for a class of PDES with random coefficients

25.2012 E. FAOU, F. NOBILE, C. VUILLOT:
Sparse spectral approximations for computing polynomial functionals

26.2012 G. ROZZA, A. MANZONI, F. NEGRI:
Reduction strategies for PDE-constrained optimization problems in haemodynamics

27.2012 C. EFFENBERGER:
Robust successive computation of eigenpairs for nonlinear eigenvalue problems

28.2012 C. LUBICH, T. ROHWEDDER, R. SCHNEIDER, B. VANDEREYCKEN:
Dynamical approximation of hierarchical Tucker and tensor-train tensors

29.2012 A. ABDULLE, Y. BAI:
Adaptive reduced basis finite element heterogeneous multiscale method

30.2012 L. KARLSSON, D. KRESSNER:
Optimally packed chains of bulges in multishift QR algorithms

31.2012 F. BONIZZONI, A. BUFFA, F. NOBILE:
Moment equations for the mixed formulation of the Hodge Laplacian with stochastic data

32.2012 M. MOTAMED, F. NOBILE, R. TEMPONE:
Analysis and computation of the elastic wave equation with random coefficients